

**An Investigation on Performance of Proton Exchange Membrane and Direct
Methanol Fuel Cells Using Taguchi Method**

By
Ng Teck Ming

Dissertation submitted in partial fulfillment of
the requirements for the
Bachelor of Engineering (Hons)
(Chemical Engineering)

SEPTEMBER 2012

Universiti Teknologi PETRONAS
Bandar Seri Iskandar,
31750 Tronoh
Perak Darul Ridzuan

CERTIFICATION OF APPROVAL

**An Investigation on Performance of Proton Exchange Membrane and Direct
Methanol Fuel Cells Using Taguchi Method**

by

Ng Teck Ming

A project dissertation submitted to the
Business Information Systems Programme
Universiti Teknologi PETRONAS
in partial fulfillment of the requirement for the
BACHELOR OF ENGINEERING (Hons)
(CHEMICAL ENGINEERING)

Approved by,

(Dr. Nooryusmiza Yusoff)

UNIVERSITI TEKNOLOGI PETRONAS
TRONOH, PERAK
September 2012

CERTIFICATION OF ORIGINALITY

This is to certify that I am responsible for the work submitted in this project, that the original work is my own except as specified in the references and acknowledgements, and that the original work contained herein have not been undertaken or done by unspecified sources or persons.

NG TECK MING

ABSTRACT

Clean and highly efficient energy development has long been sought to solve energy and environmental crisis. Fuel cells, which convert the chemical energy in fuel directly into electrical energy is the key enabling technology of this century with an excellent long-term electrochemical performance. The future energy source is concerned with two of the most advanced fuel cells – Direct Methanol Fuel Cell (DMFC) and Proton Exchange Membrane Fuel Cell (PEMFC). The focus of this work is to develop a mathematical model for investigating the best operating conditions and comparing the performance of PEMFC and DMFC. Significant results of 2D simulations conducted was expected to maximize the fuel cells' performance to be used in the transportation sector and portable applications. Two-dimensional fuel cell models were simulated based on physical laws to predict the performance of the cell under various operating conditions. Taguchi's method has been used to design experiments to study the effect of fuel and oxidant concentration, reactants' flow direction and membrane properties. Validating and running case studies of these models have been made to present a comprehensive viewpoint of modeling. Finally, comparing performance in term of current and power density between PEMFC and DMFC has been performed. PEMFC has better performance compared to DMFC.

ACKNOWLEDGEMENT

This final year project would not have been possible without the support of many people. The author wishes to express his gratitude to his supervisor, Dr. Nooryusmiza Yusoff for his patience, motivation, enthusiasm and continuous support of this 2D fuel cell simulation and research. His guidance helped the author in all the time in simulation and writing of this thesis. The author would like to express his appreciation and very special thanks to him for his guidance, support and valuable advices throughout this project.

The author also wishes to express his appreciation to all of his fellow friends, for their helps and supports throughout this project. His sincere appreciation also extends to all of his colleagues and others who have provided assistance at various occasions.

In addition, the author would also like to convey million thanks to Universiti Teknologi Petronas for providing the financial means and simulation laboratory facilities in Chemical Department.

Last but not least, the author wish to express his love and gratitude to his beloved families for their understanding and endless love, through the duration of his studies.

TABLE OF CONTENTS

CERTIFICATION	i
ABSTRACT	iii
ACKNOWLEDGEMENT	iv
CHAPTER 1: INTRODUCTION	1
1.1 Background of Study	1
1.2 Problem Statement	3
1.2.1 Problem Identification	3
1.2.2 Significance and Relevancy of the Project	4
1.3 Objective	4
1.4 Scope of Study.	4
1.5 Feasibility of the Project within the Scope and Time Frame	5
CHAPTER 2: LITERATURE REVIEW	6
2.1 Fuel Cell	6
2.1.1 Types of Fuel Cell	8
2.1.1.1 Proton Exchange Membranes Fuel Cells (PEMFC)	8
2.1.1.2 Direct Methanol Fuel Cell (DMFC)	10
2.2 Transport Mechanism in Fuel Cells	13
2.2.1 Charge Balance	13
2.2.2 Agglomerate Model for Anode and Cathode	14
2.2.3 Porous Media Fluid Flow	15
2.2.4 Maxwell Stefan Mass Transport	15
2.3 Multi-Physics 2D Fuel Cells Simulation	16
2.4 Comparison of PEMFC and DMFC	17
CHAPTER 3: METHODOLOGY	18
3.1 Methodology for Fuel Cell 2D Simulation	18
3.3 Research Methodology Method	21
3.3 Project Work	21
3.4 Design of Experiments by using Taguchi Method	22
3.5 Constants and Parameters Involved in 2D Simulation	24

3.5.1	Operating Parameters for PEMFC	24
3.5.2	Operating Parameters for DMFC	25
3.6	Experimental Tools and Software	26
3.6.1	Fuel Cell Car Toolkit	26
3.6.2	Comsol MultiPhysics Engineering Simulation Software	26
3.7	Key Milestone.	26
3.8	Gantt Chart	27
3.8.1	Gantt Chart for Final Year Project I	27
3.8.2	Gantt Chart for Final Year Project II	28
CHAPTER 4: RESULT AND DISCUSSION		29
4.1	Validation of 2D Simulated Fuel Cell Models	29
4.2	Post Processing and Visualization	31
4.2.1	Concentration Profile	31
4.2.2	Velocity Profile	31
4.2.3	Current Density Profile	31
4.3	Data Gathering and Analysis for Fuel Cells	32
4.3.1	Taguchi Table	32
4.3.2	Analysis of Means (ANOM)	32
4.3.4	Analysis of Variance (ANOVA)	34
4.3.4	Main Effect Response Plot	35
	4.3.4.1 Effect of Fuel Concentration in Anode Channel	35
	4.3.4.2 Effect of Fuel Concentration in Anode Channel	36
	4.3.4.3 Effect of Fuel Concentration in Anode Channel	37
	4.3.4.4 Effect of Fuel Concentration in Anode Channel	38
4.4	Validation for Taguchi Method	39
4.5	Comparison of PEMFC and DMFC	41
4.6	Concluding Remark	42
CHAPTER 5: CONCLUSIONS AND RECOMMENDATIONS.		43
5.1	Conclusions	43
5.2	Recommendations	44
REFERENCES		45

APPENDICES		47
A.1	Data Gathering and Analysis for PEMFC	47
A.1.1	Experiment 1	47
A.1.2	Experiment 2	47
A.1.3	Experiment 3	48
A.1.4	Experiment 4	48
A.1.5	Experiment 5	49
A.1.6	Experiment 6	49
A.1.7	Experiment 7	50
A.1.8	Experiment 8	50
A.2	Data Gathering and Analysis for DMFC	51
A.2.1	Experiment 1	51
A.2.2	Experiment 2	51
A.2.3	Experiment 3	52
A.2.4	Experiment 4	52
A.2.5	Experiment 5	53
A.2.6	Experiment 6	53
A.2.7	Experiment 7	54
A.2.8	Experiment 8	54

LIST OF FIGURES

Figure 1.1	Structural of Fuel Cell	1
Figure 2.1	Theoretical Framework and Mechanism of Fuel Cell	7
Figure 2.2	Structural of PEMFC	8
Figure 2.3	Direct Methanol Fuel Cell	10
Figure 2.4	A Schematic Diagram of DMFC Methanol Crossover Process	12
Figure 2.5	Mechanism of DMFC	12
Figure 3.1	2D Simulation Methodology	18
Figure 3.2	Model Geometry with Equations, Subdomain and Boundary Labels	19
Figure 3.3	Concentration, Velocity and Current Density Profile	20
Figure 3.4	Flow Diagram of Taguchi Method	22
Figure 3.5	Direct Methanol and Proton Exchange Membrane Fuel Cells	26
Figure 3.6	Key Milestone	26
Figure 3.7	Gantt Chart for Final Year Project I	27
Figure 3.8	Timeline for Final Year Project II	28
Figure 4.1	Polarization Curve of DMFC	31
Figure 4.2	Temperature Profile for PEMFC	30
Figure 4.3	Concentration, Velocity and Current Density Profiles	31
Figure 4.4	Result summarize in Taguchi Method	32
Figure 4.5	ANOM Plot	33
Figure 4.6	Main Effect Response Plot	35
Figure 4.7	Methanol Concentration Profile in DMFC	36
Figure 4.8	Oxygen Concentration in PEMFC and DMFC	37
Figure 4.9	Directional Flow Profile in PEMFC and DMFC	37
Figure 4.10	Type of Nafion Membrane Profile	39
Figure 4.11	Fuel Cell Performance graph for PEMFC and DMFC	41
Figure 5.1	Fuel Cell Performance Pie Chart for PEMFC and DMFC	43

LIST OF TABLES

Table 2.1	Comparison between PEMFC & DMFC	17
Table 3.1	L ₈ Taguchi Method in 2D Fuel Cell Simulation	23
Table 3.2	Constants Used in 2D PEMFC Model Simulation	22
Table 3.3	Constants Used in 2D DMFC Model Simulation	23
Table 4.1	ANOM Table for PEMFC	33
Table 4.2	ANOM Table for DMFC	33
Table 4.3	ANOVA Table for PEMFC	34
Table 4.4	ANOVA Table for DMFC	34
Table 4.5	Comparison between Membranes	38
Table 4.6	Validation Table for PEMFC	40
Table 4.7	Validation Table for DMFC	40
Table 5.1	Conclusion remark for PEMFC and DMFC	43

ABBREVIATIONS AND NOMENCLATURES

FE-DMFC	Flowing Electrolyte- Direct Methanol Fuel Cell
ADL	Anode Diffusion Layer
ACL	Anode Catalyst Layer
CDL	Cathode Diffusion Layer
CCL	Cathode Catalyst Layer
PEM	Polymer Electrolyte Membrane
MEA	Membrane Electrode Assembly
Ω_A	Anode's Domain
Ω_C	Cathode's Domain
A	Ampere (<i>I</i>)
CC	Current Collector
CH ₃ OH	Methanol
C _{CH₃OH}	Concentration of Methanol
C _k	Percentage contribution of factor k
V _k	Variance of factor k
\bar{X}	Average of current density
\bar{X}_k	Average of profit due to factor k over all 2 levels
\bar{X}_{k1}	Average of profit due to factor k at level 1
\bar{X}_{opt}	Optimal current density

CHAPTER 1

INTRODUCTION

1.1 Background of Study

The fuel cell is a device that transforms the chemical energy from a fuel into electricity through a chemical redox reaction with oxygen or other oxidizing agent. Hydrogen is the most common fuel, but hydrocarbons such as natural gas and alcohols like methanol are frequently used. Fuel cells are different from batteries in that they require a constant source of fuel and oxygen to run, but they can produce electricity continuously for as long as these inputs are supplied.

Welsh Physicist William Grove developed the first crude fuel cells in 1839. The first commercial use of fuel cells was in NASA space programs to generate power for probes, satellites and space capsules. Since then, fuel cells have been used in many other applications. Fuel cells are used for primary and backup power for commercial, industrial and residential buildings and in remote or inaccessible areas (Grove, 1842). Fuel cells produce water and heat. The energy efficiency of a fuel cell is generally between 40–60%, or up to 85% efficient if waste heat is captured for use. It is much higher than a combustion engine, which is generally 30% efficient.

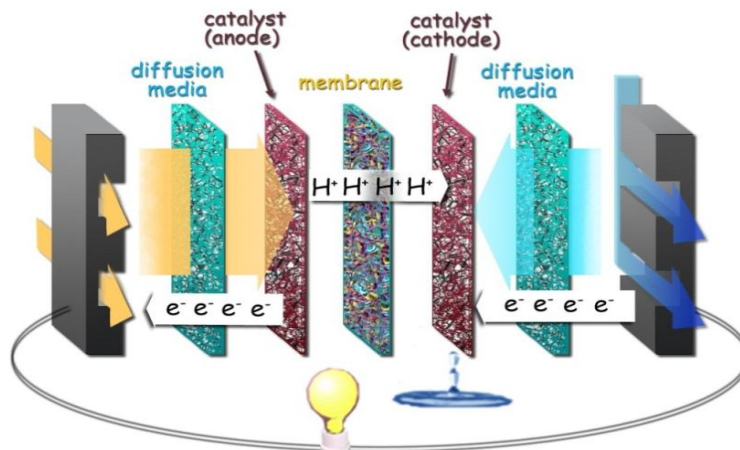


Figure 1.1: Structural of Fuel Cell (Source: Environmental Energy Technologies Division (EETD))

Figure 1 shows the internal component of a fuel cell and how a fuel cell will work. Hydrogen (yellow) fed into the cell diffuses to the anode catalyst and reacts to form protons and electrons. The protons travel through the membrane, while the electrons form a current in an external circuit. Meanwhile, oxygen (blue) from air diffuses to the cathode catalyst layer, where it reacts with protons that have crossed the barrier and electrons arriving from the circuit, to form water, current density and heat.

Fuel cells are considered as green, reliable and highly efficient power generation technology in future. Among various types of fuel cells, Proton Exchange Membrane (PEMFC) and Direct Methanol Fuel Cells (DMFCs) are commonly used because of low weight, high energy density, simple design, low CO₂ emission and safety of fuel handling properties. These are the most promising power sources for portable electronic devices and transportation applications (C. Siegel, 2008). It has been shown that Nafion membrane is able to provide selective and high permeability to water and small cations, such as protons. However, expensive cost is the critical limitations of Nafion membrane for DMFC and the high flammability of Hydrogen fuel in PEMFC. In recent years, significant progress has been made to develop polymer electrolyte membranes for DMFC in terms of reduced cost as well as improved functionality.

The necessary improvements in fuel cell operation and performance demands better design and optimization. These issues can be addressed easily if mathematical models are available. Traditionally the flow field plates are made of graphite and the current collection is carried out from the flow field plates. But in literature, many authors have reported building micro fuel cells, where the flow field plates are also made of silicone. The channel width plays an important role in the performance of micro fuel cells. Here the channel width is varied from 0.5 mm to 1.5 mm and the performance variation is studied.

Flow direction of reactant in fuel cells also one of the important parameters that can affect the performance of fuel cells in term of current density (A.m⁻²). In most of the journal papers, magazine and research studies shown that PEMFC uses concurrent flow and the performance is not that efficient compare to counter current flow of the

reactant. In fuel cells, the two reactants enter at the same end, and transfer in parallel to another from another side. In counter-flow fuel cells, the reactants enter from opposite ends. The maximum amount of heat or mass transfer that can be obtained is higher with countercurrent than concurrent (parallel) because countercurrent maintains a slowly declining difference or gradient (usually temperature or concentration difference).

Generally, the fuel concentration in the anode and oxidant concentration in cathode affects the performance of a fuel cell. By using a higher concentration of fuel in anode channel and higher oxidant concentration in cathode channel can produce higher current density. It is because higher concentrations of fuel in anode can produce many hydrogen protons from Anode catalyst layer and then the protons will pass through the membrane and reach the cathode to react with oxygen to form electricity and water. Besides that, higher oxidant concentration in the cathode can accelerate the chemical redox reaction in a fuel cell to yield higher current density. It is because the hydrogen ion that reached cathode can fully react with oxygen ion in cathode to yield optimum current density.

1.2 Problem Statement

1.2.1 Problem Identification

Recently, there has been a rising concern about acid rain and greenhouse gas emissions which have made renewable technologies an attractive option. In an ongoing effort to meet increasing energy demand and also to preserve the global environment, the development of fuel cell energy systems with readily available fuels, high efficiency and minimal environmental impact is urgently required. PEMFC and DMFC are among the fuel cells which are most commonly used in the current century. But the problem rising now is low performance in term of current density ($A.m^{-2}$) produced by PEMFC and DMFC.

In fact, it can be maximized by manipulating operating parameters and design system variables simultaneously. These variables/parameters can be classified into two which are process variable and design variable in fuel cells. Process variable

includes of direction flow of reactants, pressure and velocity of reactants flow, operating temperature, fuel cell's structure and so on. While design variable includes of channel length and width, different type and porosity of membrane used and other design variations of fuel cells as well. Hence, 2D simulated models of PEMFC and DMFC were simulated in this work to select the best operating parameter and design variable to deliver the best performance of a fuel cell system using Taguchi's Method.

1.2.2 Significance and Relevancy of the Project

The significance of this project is that, with the 2D models simulated, developer can identify and apply the best operating condition and the most suitable design variable on a fuel cell. In this work, Taguchi's method and main effect response plot have been used to study and investigate the effects of different parameter in order to maximize the current density of the fuel cell. These process and system variables include of fuel and oxidant concentration, directional flow of reactant and membrane properties. By creating a 2D simulated model of PEMFC and DMFC in Comsol MultiPhysics, those processes and design variables can be easily optimized to produce the maximum current density. By using response plot, main effects of certain parameter can be determined to a fuel cell's performance.

1.3 Objective

The objective to be achieved in this project is to maximize the current density by investigating effects of fuel and oxidant concentration, membrane properties and direction flow of reactants in fuel cells using Taguchi's Method.

1.4 Scope of Study

The scope of study of this project is encircled around the current density produced by PEMFC and DMFC. Besides that, a study regarding the mechanism of a fuel cell system and simulating 2D fuel cell models in Comsol MultiPhysics. Therefore, besides understanding the mechanism of a fuel cell by running some case studies, the scope of study for this project also involves validating 2D fuel cell models with experimental data done previously by researchers and validation of Taguchi Method.

Furthermore, there is a fuel cell toolkit that can be used for validation purpose and to investigate the effects of those processes and design variables (fuel and oxidant concentration, membrane properties and direction flow of reactants in fuel cells).

1.5 Feasibility of the Project within the Scope and Time Frame

Feasibility analysis was conducted to determine the simulation tools which would be used throughout the development of 2D simulated fuel cell models. Since there are several types of simulation tools such as Matlab, Computational Fluid Dynamics Software (CFD), Ansys Fluent Flow Modeling Simulation Software and Comsol. Comsol MultiPhysics Engineering Simulation Software was selected for 2D simulation of fuel cell in this work. It is because Comsol MultiPhysics is more advanced and more user friendly simulation environment.

In addition, since final year project consist of part one and part two, it is important to ensure that sufficient research work and literature review have been done in the first part of the final year project and 2D fuel cell models can be successfully simulated, validated and optimized within the stated timeline for the second part of the final year project.

In short, the deliverables for final year project one and final year project two should be ready upon the completion of both semesters of final year project, respectively.

CHAPTER 2

LITERATURE REVIEW

In this chapter, theoretical framework and mechanism of Proton Exchange Membrane and Direct Methanol Fuel Cells were being reviewed from previous research journal papers. Most frequently used fuel cell in the worldwide today with the advantages of a low operating temperature and fast startup for transportation and residential power applications. Further advantages include there are no corrosive fluid and emission hazards in fuel cell hence it can work in any environment. Besides that, some simulation work about fuel cells has been reviewed in this chapter.

2.1 Fuel Cell

A **fuel cell** is a device that transforms the chemical energy from a fuel into electricity through a chemical reaction with oxygen or other oxidizing agent. Hydrogen is the most common fuel, but hydrocarbons such as natural gas and alcohols like methanol are sometimes used. Fuel cells are unlike from batteries in that they involve a constant source of fuel and oxygen to run, but they can yield electricity continuously for as long as these inputs are supplied. Welsh Physicist William Grove developed the first crude fuel cells in 1839. The first commercial use of fuel cells was in NASA space programs to generate power for probes and satellites (William Grove, 1839).

There are numerous types of fuel cells, but they all consist of an anode (negative side), a cathode (positive side) and an electrolyte that allows electron to travel between the two sides of the fuel cell. Catalyst oxidizes the fuel at anode, usually hydrogen or other hydrogen compound, turning the fuel into a positively charged ion and a negatively charged electron. The electrolyte is a substance specifically designed so ions can pass through it, but the electrons cannot. Electrons are drawn from the anode to the cathode through an external circuit, producing direct current

electricity. Two chemical redox reactions occur at the interfaces of the three different sectors. The net result of the two reactions is that fuel is consumed, water or carbon dioxide (DMFC) is formed, and an electric current is produced, which can be used to power electrical devices as indicated in figure 2.1 below.

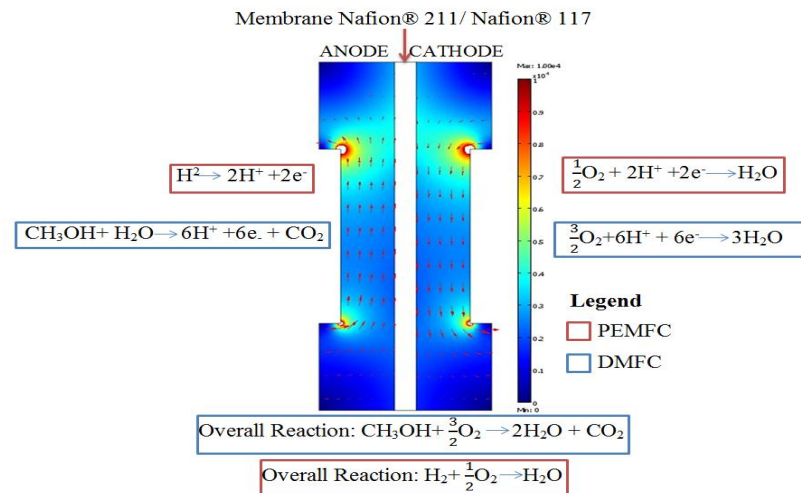


Figure 2.1: Theoretical Framework and Mechanism of Fuel Cell

For PEMFC, half reaction in anode is breaking the hydrogen molecule down to hydrogen ion and electron charges. Hydrogen is broken down by using platinum catalyst. The main concern in a fuel cell is the price of the platinum is too high. Because of this issue, fuel cell cannot be fully commercialized in the current century. Many researches have been done by researchers worldwide and cheaper organic polymer membrane has been invented to solve this issue. Then, hydrogen ion diffuses through the membrane to cathode channel and combines with oxygen to form electricity, water and heat. The overall reaction of the PEMFC is hydrogen react with oxygen to form water. PEMFC consider clean energy because release no carbon dioxide and other global warming gases.

For DMFC, methanol will break down to release 1 mole of carbon dioxide and hydrogen ion will pass through the membrane to cathode channel. It will combine with oxygen to form water as shown in stoichiometry equation in figure above. The overall reaction of DMFC is 1 mole of methanol reacts with 1.5 moles oxygen to form water and 1 mole of carbon dioxide. DMFC only release 1 mole of carbon dioxide from 1 mole of methanol. The amount of carbon dioxide released from DMFC is 8 times lesser than normal combustion engine which uses octane fuel (C_8H_{18}).

Application of fuel cell can be concluded as below:

a.) Emergency power systems

Emergency power systems are a type fuel cell system, which may include lighting, generators and other apparatus, to provide backup resources in a crisis or when regular systems fail. (C.K. Dyer, 2002).

b.) Uninterrupted Power Supply (UPS)

UPS provides emergency power from a separate source when utility power is not available. Usually used are hospital and some government agencies.

c.) Cogeneration

Cogeneration can be used when the fuel cell is sited nearby. Its waste heat can be captured for beneficial purposes include of heating, ventilation and air conditioning (HVAC) in the building.

d.) Portable Power Systems

Portable power systems that use fuel cells, can be used in the leisure sector (Cabins & Marine), the industrial sector (power for remote locations including gas/oil well sites, communication towers, weather stations), or in the military sector. SFC Energy is a German manufacturer of direct methanol fuel cell, which uses their fuel cell for a variety of portable power systems.

2.1.1 Types of Fuel Cell

2.1.1.1 Proton Exchange Membranes Fuel Cells (PEMFC)

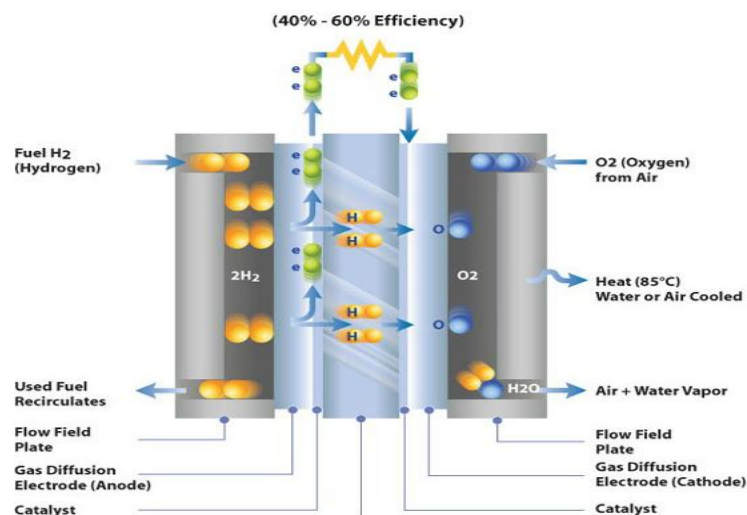


Figure 2.2: Structural of PEMFC (Source: Australian Ballard Power Systems)

PEMFC is an attractive alternative energy sources for transportation, stationary power, and small electronics due to the increasing cost and environmental hazards of traditional fossil fuels. Ideal PEMFC should have good thermal, hydrolytic, and oxidation stability, high proton conductivity, selective permeability, and mechanical durability over long periods of time (Mohammad Mahdi Hasani-Sadrabadi, 2010).

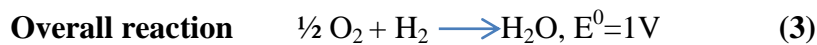
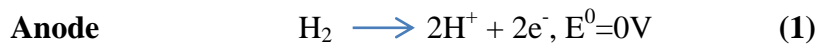
On the anode side, hydrogen diffuses to the anode catalyst where it later separates into protons and electrons. These protons often react with oxidants and causing them to become what is commonly referred to as multi-facilitated proton membranes. The protons are conducted through the membrane to the cathode, but the electrons are forced to travel in an external circuit (supplying power) because the membrane is electrically insulating. On the cathode catalyst, oxygen molecules react with the electrons (which have traveled through the external circuit) and protons to form water. The only waste product is either liquid or vapor (H_2O).

Introduction of an inorganic component into proton exchange membranes can further improve the properties by potentially decreasing the water while increasing the modulus and mechanical strength of the membrane. Metal oxides, phosphates, and phosphonates are among the most common additives employed in fuel cell membranes. Several challenges for the PEMFC power technology are associated with low operating temperature. Fuel processors for example hydrogen storage tanks and hydrocarbon or alcohol reformers with subsequent CO removers are voluminous, heavy, costly and in most cases complex (O. Lottin, 2007). Water management involves appropriate humidification of fuel and oxidant, airflow rate and power load regulation. Temperature control or cooling is more critical for larger stacks and the heat is of low value. (S. Basri, 2011).

A fuel cell-powered car can run for longer distances with the same amount of fuel compared to a conventional car. Carbon dioxide emissions are consequently lowered, because smaller amounts of fuel are consumed for the

same distance traveled. In addition, the low temperatures in the process practically eliminate the production of NO_x and SO_x . Electrons are released to an outer circuit at the anode, and they are received through the same circuit at the cathode. The electronic current is transported to and from the electrodes through the gas backing to the current collector and then to the outer electrical circuit. There is also an ionic current of protons running from the anode to the cathode through the electrolyte.

Redox Reaction in PEMFC



2.1.1.2 Direct Methanol Fuel Cell (DMFC)

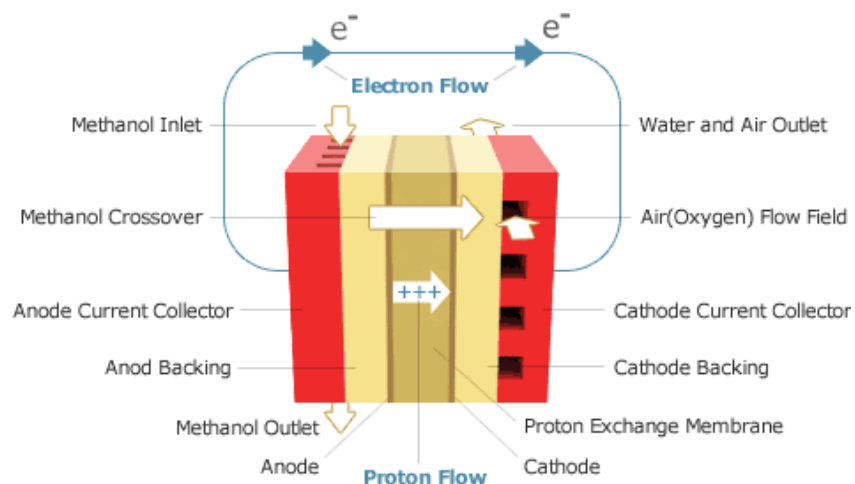


Figure 2.3: Direct Methanol Fuel Cell (Source: Sympowercorp)

Direct Methanol Fuel Cell (DMFC) is an electrochemical energy conversion device that transforms chemical energy of liquid methanol into electrical energy directly as shown in figure 2.3. Because of its unique advantages, such as higher energy densities, superficial liquid fuel storage, and simpler system structures, the DMFC has been identified as one of the most promising power sources for portable and mobile applications (S.C. Thomas, 2002). DMFC is clean and highly efficient energy production and has long been sought to solve energy and environmental problems. Electrons are released to an outer circuit at the anode, and they are received through the same circuit at the cathode. The electronic current is transported to and from

the electrodes through the gas backing to the current collector and then to the outer electrical circuit. There is also an ionic current of protons running from the anode to the cathode through the electrolyte.

DMFC use a methanol solution (usually around 1M or about 3% in mass) to carry the reactant into the cell. Common operating temperatures are in the range 50–120 °C, where high temperatures are usually pressurized. DMFCs are more efficient at high temperatures and pressures, but these conditions will cause many losses in fuel cell system (S.K. Kamarudin, 2006).

Kamarudin et al. [13] discussed in their review paper that the combination of DMFC with thin film batteries (i.e. A hybrid power system) is one of the possible short-term solutions to overcome the economic issues associated with DMFC. In addition to controlling the operating parameters and the search in the alternative materials, new configurations and designs have been also proposed to increase the performance of the DMFC. The Flowing Electrolyte-DMFC, which was proposed by T.S. Zhao [15], is a novel DMFC design which provides performance improvement by eliminating the methanol crossover from the anode to the cathode.

Single DMFC that consists of a membrane electrode assembly (MEA) sandwiched by anode and cathode bipolar plates with the machined flow fields. The MEA is a multi-layered structure that is composed of an anode diffusion layer (ADL), an anode catalyst layer (ACL), a polymer electrolyte membrane (PEM), a cathode diffusion layer (ADL), and a cathode catalyst layer (CCL). The function of the membrane is to conduct protons from the anode to the cathode. Mass Transport Phenomena including the reactants (methanol, oxygen and water) and the products (water and carbon dioxide) in DMFCs (Larminie J, Dicks, 2003).

Figure 2.4 shown methanol crossover phenomenon by which methanol diffuses through the membrane without reacting with air, methanol is fed as a

weak solution. This decreases efficiency significantly, since crossed-over methanol, after reaching the air side (the cathode), immediately reacts with air; though the exact kinetics are debated, the end result is a reduction of the cell voltage. Crossover remains a major factor in inefficiencies, and often half of the methanol is lost to cross over (T.S. Zhao, 2007).

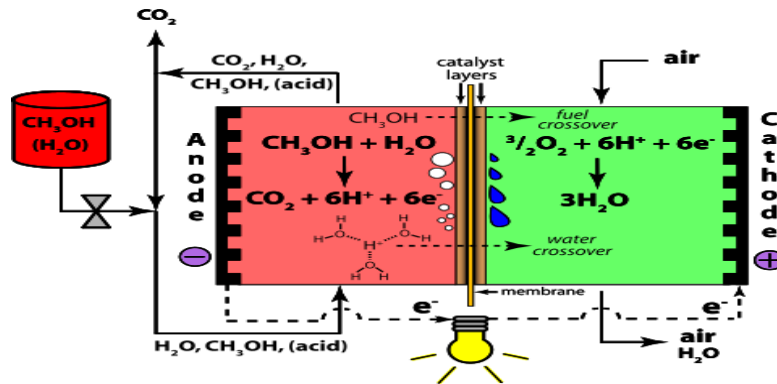


Figure 2.4: A Schematic Diagram of DMFC Methanol Crossover Process (Source: http://www.wpclipart.com/science/how_things_work/Direct_Methanol_Fuel_Cell__Methanol_and_Water_Crossover.png.html)

Other issues include the management of carbon dioxide created at the anode, the sluggish dynamic behavior, and the ability to maintain the solution water. The only waste products with these types of fuel cells are carbon dioxide and water (V.S. Silva, 2005).

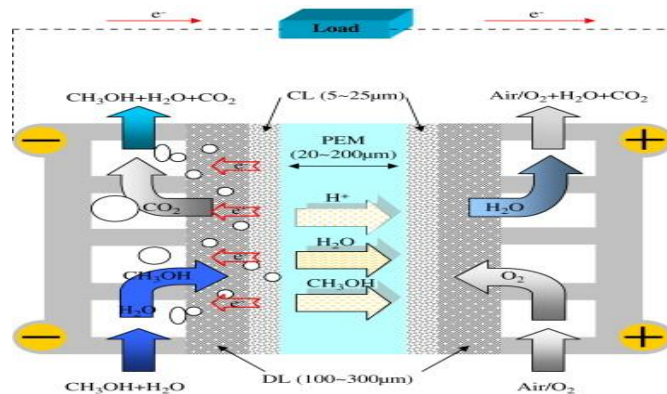
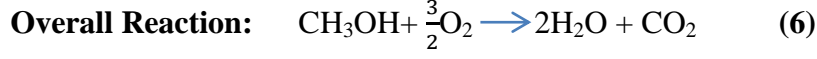
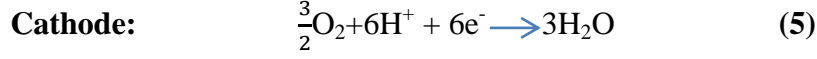
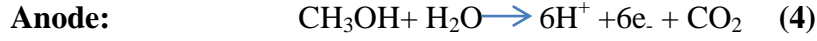


Figure 2.5: Mechanism of DMFC (Source: Sympowercorp)

From figure 2.5 above, there is a mechanism of DMFC where methanol and water are adsorbed on a catalyst usually made of platinum and ruthenium particles, and lose protons until carbon dioxide is formed. As water is consumed at the anode in the reaction, pure methanol cannot be used without provision of water via either passive transport such as back diffusion (osmosis), or active transport such as pumping. The need for water limits the current density of the fuel. The DMFC relies upon the oxidation of methanol

on a catalyst layer to form carbon dioxide. Protons (H^+) transport across the membrane.



2.2 Transport Mechanism in Fuel Cells

At the cathode, oxygen reacts together with the protons to form water in the active layer. Both feed gases (humified hydrogen and humidified air) are treated as ideal and are transported through diffusion and convection. The electrodes are treated as homogeneous porous media with uniform morphological properties such as porosity and permeability. The gas within each of the electrodes exists as a continuous phase so Darcy's law applies (C. Ozgur Colpan, 2012). At the anodic active catalyst layer, hydrogen is the diffusing and reacting species in the agglomerates, while oxygen is the diffusion and reacting species in the agglomerates at the cathode. An agglomerate model of the cathode active catalyst layer of a PEM fuel cell has been presented by Brooke and others.

2.2.1 Charge Balance

A Conductive Media DC application mode describes the potential distributions in the three subdomains using the following equations:

$$\nabla \cdot (\mathbf{\kappa}_{s, \text{eff}} \nabla \phi_s) = 0 \text{ in } \Omega_a \quad (7)$$

$$\nabla \cdot (\mathbf{\kappa}_{m, \text{eff}} \nabla \phi_m) = 0 \text{ in } \Omega_m \quad (8)$$

$$\nabla \cdot (\mathbf{\kappa}_{s, \text{eff}} \nabla \phi_s) = 0 \text{ in } \Omega_c \quad (9)$$

Here $\kappa_{s, \text{eff}}$ is the solid-phase effective electronic conductivity (S/m) and $\kappa_{m, \text{eff}}$ is the membrane ionic conductivity (S/m). The potential (V) in the electrode phases is denoted by ϕ_s and that in the membrane by ϕ_m .

Charge transfer current density expression generally described by using the Butler-Volmer electrochemical kinetic expression as a boundary condition. For the electrolyte potential equation, this results in a condition where the inward

normal Ionic current densities at the anode and cathode boundaries, I and I_{ke} , are specified according to the equation below:

$$i_e = L_{act} (1 - \epsilon_{mac}) j_{agg, e} \quad (10)$$

Where: e - ‘‘a’’ (anode) or ‘‘c’’ (cathode)

L_{act} - active layer’s thickness (m)

ϵ_{mac} - porosity (the macroscopic porosity)

$j_{agg, a}$ and $j_{agg, c}$ - current densities given by the agglomerate model

2.2. 2 Agglomerate Model for Anode and Cathode

Current density can be expressed analytically by solving a combination of the Maxwell Stefan Diffusion equation and the Butler-Volmer electrode kinetic equation for agglomerate with constant electric and ionic potentials. The resulting equations for the current density in the anode and cathode are:

$$j_{agg, e} = -6n_e F \left(\frac{D_{agg}}{R_{agg}^2} \right) (1 - \lambda_e \coth \lambda_e) \beta_e \quad (11)$$

$$\lambda_a = \sqrt{\frac{i_{0a} S R_{agg}^2}{2F c_{H_2, ref} D_{agg}}} \quad \lambda_c = \sqrt{\frac{i_{0c} S R_{agg}^2}{4F c_{O_2, ref} D_{agg}} \exp\left(-\frac{F}{2RT} \eta_c\right)} \quad (12)$$

$$\beta_a = \left[c_{H_2, ref} - c_{H_2, ref} \exp\left(\frac{-2F}{RT} \eta_a\right) \right] \quad \beta_c = c_{O_2, agg} \quad (13)$$

Where: D_{agg} Agglomerate gas diffusivity ($m^2 \cdot S^{-1}$)

R_{agg} Agglomerate radius (m)

n_e ‘‘charge transfer’’ number (1 for the anode and -2 for the cathode)

S Specific area of the catalyst inside the agglomerate (m^{-1})

F Faraday’s constant ($C \cdot mol^{-1}$)

$c_{i, ref}$ Reference concentrations of the species ($mol \cdot m^{-3}$)

$c_{i, agg}$ Concentrations of agglomerate surface ($mol \cdot m^{-3}$)

R Gas constant

T Temperature (K)

i_{0a} and i_{0c} are the exchange current densities ($A \cdot m^{-2}$)

The dissolved hydrogen and oxygen concentrations at the surface of the agglomerates are related to the molar fractions of the respective species in the gas phase through Henry’s law.

$$c_{agg, H_2} = \frac{p_H x_H}{K_H}$$

$$c_{agg, O_2} = \frac{p_O x_O}{K_O} \quad (14)$$

Where K is Henry's constant ($\text{Pa}\cdot\text{m}^3\cdot\text{mol}^{-1}$). The potential difference between the cathode and anode current collectors corresponds to the total cell voltage. Then the total cell voltage serves as the boundary condition at the cathode current collector:

$$\begin{aligned}\varphi_s &= 0 \text{ at } \partial\Omega_{a, cc} \\ \varphi_s &= V_{\text{cell}} \text{ at } \partial\Omega_{c, cc}\end{aligned}\quad (15)$$

2.2.3 Porous Media Fluid Flow

Darcy's Law was being applied in simulation to indicate the fluid flow through a porous medium. The gas velocity is given by the continuity equation as below:

$$\nabla \cdot (\rho\mathbf{u}) = 0 \text{ in } \Omega_a \text{ and } \Omega_c \quad (16)$$

Where ρ is the mixture density of the gas phase ($\text{kg}\cdot\text{m}^{-3}$) and \mathbf{u} denotes the gas velocity ($\text{m}\cdot\text{s}^{-1}$). Darcy's law for porous media states that the gradient of pressure, the viscosity of the fluid, and the structure of the porous media determine the velocity:

$$\mathbf{u} = kp/\eta \cdot \nabla p \quad (17)$$

Where: kp electrode's permeability (m^2)
 η gas viscosity ($\text{Pa}\cdot\text{s}$)
 p pressure (Pa)

2.2.4 Maxwell Stefan Mass Transport

There are H_2 and H_2O at Anode side and O_2 , H_2O , and N_2 at the cathode side. The equations that describe these transport processes have been developed independently and in parallel by James Clerk Maxwell for dilute gases and Josef Stefan for fluids. Maxwell-Stefan multicomponent diffusion of each electrode is governed by the equations as shown below:

$$\frac{\partial}{\partial t}\rho w_i + \nabla \cdot \left[-\rho w_i \sum_{j=1}^N D_{ij} \left\{ \frac{M}{M_j} \left(\nabla w_j + w_j \frac{\nabla M}{M} \right) + (x_j - w_j) \frac{\nabla p}{p} \right\} + w_i \rho \mathbf{u} + D_i \frac{T \nabla T}{T} \right] = R_i \quad (18)$$

Here p is the pressure (Pa), \mathbf{u} is the velocity ($\text{m}\cdot\text{s}^{-1}$), and D_{ij} is Maxwell-Stefan diffusivity matrix ($\text{m}^2\cdot\text{s}^{-1}$), M is the concentration of species ($\text{Mol}\cdot\text{L}^{-1}$), w is the mole fraction while x is mole fraction of the species.

2.3 Multi-Physics 2D Fuel Cells Simulation

Multi-physics simulations based on multi-component multi-solver modeling approach were performed for fuel cells. Simulations of fuel cells were performed using a combined transport solver in multi-species environment. The component included the structure (anode, cathode, and electrolyte), air/fuel channels and ambient environments. Species concentrations, mass, momentum, energy fluxes, and electric potentials were solved for different components. Models for unsteady fluid dynamics of the species, heat transport, electrochemistry and electric currents were combined within different components and inter-component boundaries. The main assumptions used in the modeling are as follows (F. Hamdullahpur, 2012):

- a) The formations of the CO₂ bubbles and water vapor are neglected. Two phase effects are not taken into account.
- b) Membranes are fully hydrated.
- c) Methanol in DMFC is fully consumed at the interface of the cathode membrane and the cathode catalyst layer.
- d) The flow in the electrolyte channel is considered as a fully developed laminar flow.
- e) The fuel cell is isothermal and operates at the steady state condition.

Mass conservation or the continuity equation says that the change of mass in a unit volume must be equal to the sum of all species entering or exiting the volume in a given time period. This law applies to the flow field plates, GDL and the catalyst layer. Momentum conservation relates the net rate of change of momentum per unit volume due to convection, pressure, viscous friction and pore structure. This law applies to the flow field plates, GDL and the catalyst layer. Species conservation relates the net rate of species mass change due to convection, diffusion and electrochemical reaction. The most commonly used one is the Stefan-Maxwell diffusion equation. Charge conservation corresponds to the continuity of current in a conducting material. This is applied to the GDL, catalyst layer and the membrane.

2.4 Comparison of PEMFC and DMFC

PEMFC is different in some ways than DMFC although both of them use hydrogen fuel to generate electricity and water as a byproduct. PEMFC use hydrogen fuel while DMFC use methanol. PEMFC has higher current and power density than DMFC while methanol fuel is easy to be stored in DMFC than hydrogen fuel in PEMFC. A detailed comparison of both fuel cells as shown in table 2.1 below.

Table 2.1: Comparison between PEMFC & DMFC

Aspect	PEMFC	DMFC
Fuel	- Hydrogen	- Methanol (CH ₃ OH)
Advantages	<ul style="list-style-type: none"> - High power density & energy efficiency - Low temperature of operating condition 	<ul style="list-style-type: none"> - High power density - Fuel can be handled, stored and transported similarly to conventional liquid fuels - System simplicity
Disadvantages	<ul style="list-style-type: none"> - Cost Effectiveness - Water management - Heat losses 	<ul style="list-style-type: none"> - Methanol is poisonous and corrosive. - Methanol crossover - Low electrical efficiencies
Applications	- Hybrid power bus, bicycle, power generator and PC.	- Electric motors, portable electricity supply, battery substitute.

CHAPTER 3

METHODOLOGY

3.1 Methodology for Fuel Cell 2D Simulation

The methodology that will be used in developing this system is the 2D Simulation Methodology as shown in the **Figure 3.1** below.

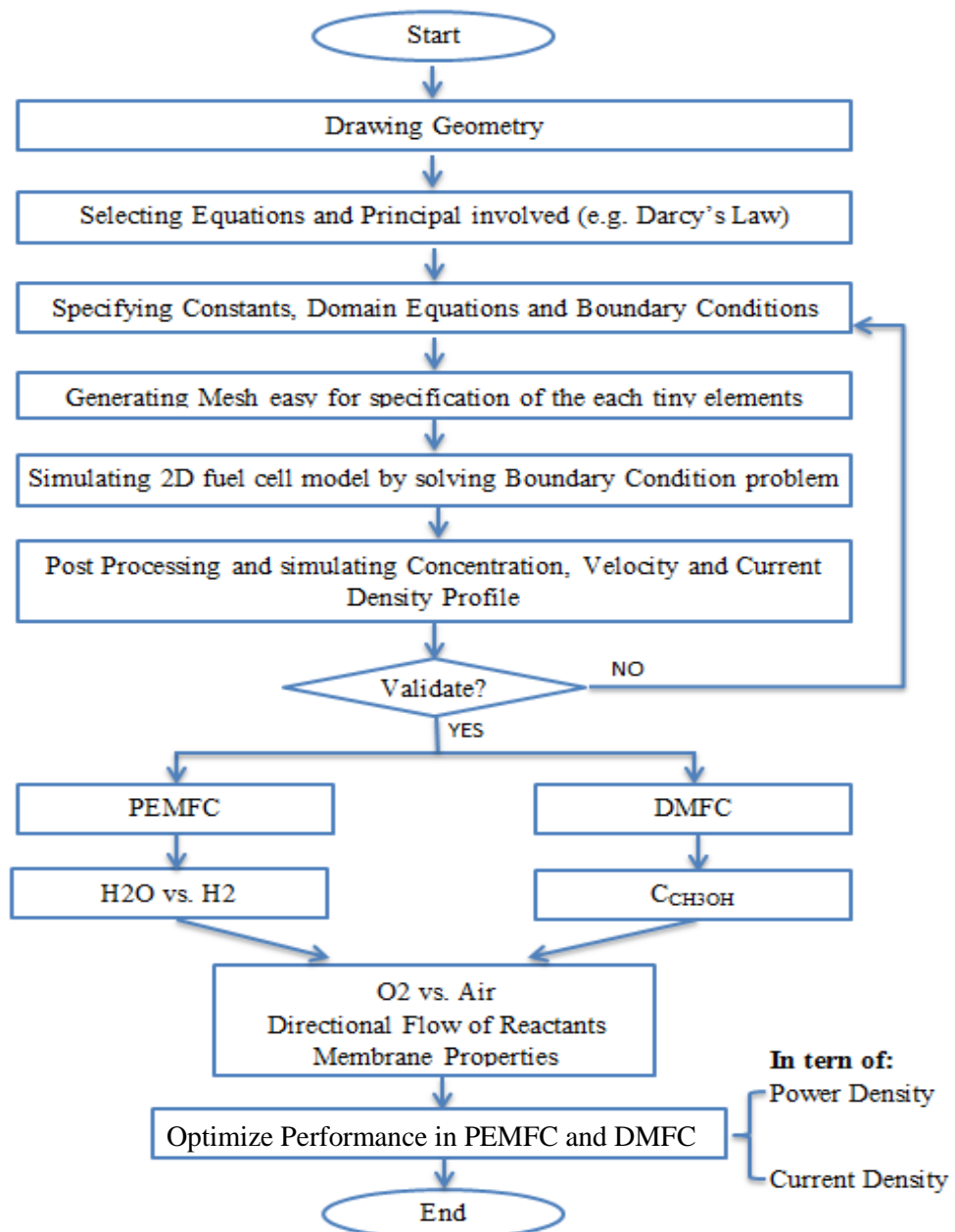


Figure 3.1: 2D Simulation Methodology

From the figure 3.1, it is a symmetric 2D simulation flow diagram of a fuel cell. This methodology enables the developer to quickly simulate a 2D fuel cell model in any engineering simulation software. In this work, 2D models were simulated in Comsol MultiPhysics version 3.5a.

First of all, fuel cell geometry has been drawn in Comsol. A set of equations involved in this 2D simulation has been nominated such as Darcy's Law (flow of fluid through a porous medium), Maxwell Stefan Mass Transport Equation (diffusion in multicomponent systems), Ohm's Law (current through a conductor between two points is directly proportional to the potential difference across the two points), Henry's Law (at a constant temperature, the amount of gas that dissolves in liquid is directly proportional to the partial pressure of that gas) and Butler Volmer Kinetics Electrochemical Kinetic Expression used as a boundary condition.

Next, constants, domain equations and boundary conditions involved in this simulation were specified as indicated in figure 3.2. This model consists of 3 domains which is an anode (Ω_a), membrane (Ω_m), and a cathode (Ω_c). Each of the porous electrodes is in contact with a gas distributor, which has an inlet channel ($\partial\Omega_a$, inlet), a current collector ($\partial\Omega_a$, cc), and an outlet channel ($\partial\Omega_a$, outlet). The same notation is used for the cathode side.

Maxwell-Stefan Diffusion

$$\frac{\nabla \mu_i}{RT} = \nabla \ln a_i = \sum_{\substack{j=1 \\ j \neq i}}^n \frac{\chi_i \chi_j}{\mathcal{D}_{ij}} (\vec{v}_j - \vec{v}_i) = \sum_{\substack{j=1 \\ j \neq i}}^n \frac{c_j c_j}{c^2 \mathcal{D}_{ij}} \left(\frac{\vec{J}_j}{c_j} - \frac{\vec{J}_i}{c_i} \right)$$

Butler-Volmer Kinetic

$$j_{agg,e} = -6n_e F \left(\frac{D_{agg}}{R_{agg}^2} \right) (1 - \lambda_e \coth \lambda_e) \beta_e$$

Darcy's Law

$$\nabla \cdot (\rho \mathbf{u}) = 0 \text{ in } \Omega_a \text{ and } \Omega_c$$

$$\mathbf{u} = -\frac{k_p}{\eta} \nabla p$$

- κ_s - effective electronic conductivity (S/m)
- j_{agg} - current density (A/m²)
- ϵ_{mac} - porosity
- L_{act} - active layer's thickness (m)
- Φ - Potential (V)
- F - Faraday's Constant (C/mol)
- n_e - charge transfer number
- k_p - electrode's permeability (m²),
- η - Gas viscosity (Pa·s)
- D_{agg} - agglomerate gas diffusivity (m²/s)
- R_{agg} - agglomerate radius (m)
- λ - excess reactant
- β - Apparent Charge Transfer coefficient

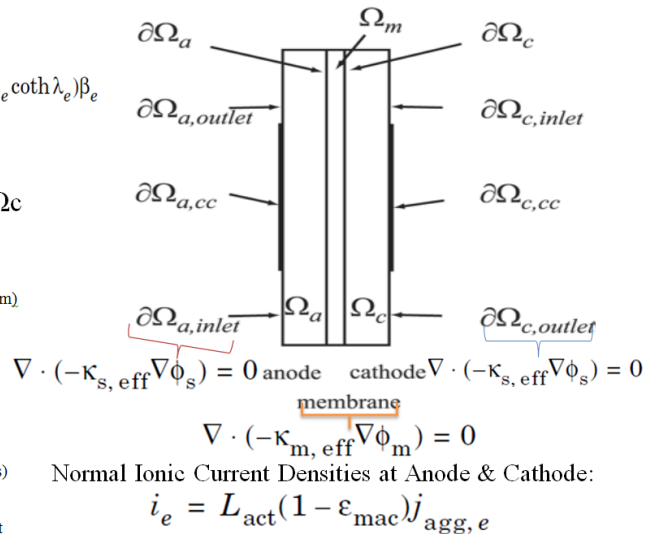


Figure 3.2: Model Geometry with Equations, Subdomain and Boundary Labels

After specifying constants, domain equations and boundary condition of fuel cell, a mesh model has been generated easy for the specification of each tiny element in this mesh. In this work, maximum element size for membrane is 50 μm and for both anode and cathode is 10 μm .

After the fuel cell model has been meshed, a 2D fuel cell model was simulated by solving the boundary condition. Three profiles which are Concentration, Velocity and Current Density profile will be simulated and post processing as shown in figure 3.3 below. Further explanation of these three profiles will be discussed in Chapter 4.

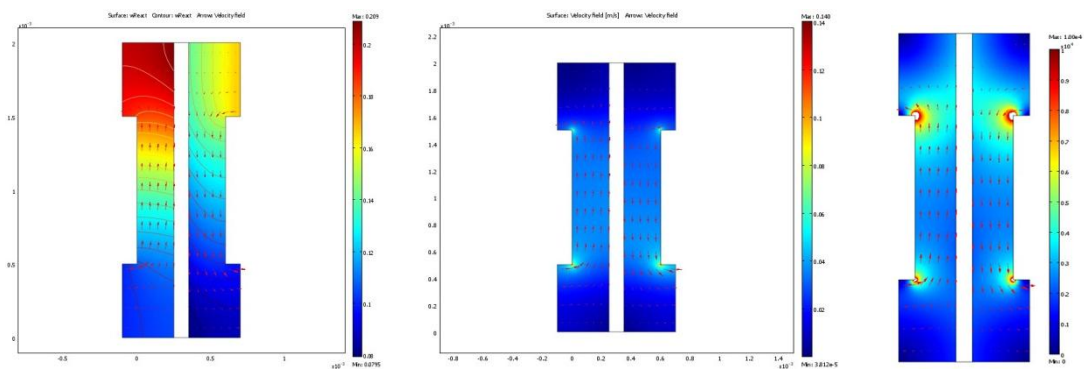


Figure 3.3: Concentration, Velocity and Current Density Profile

The following step in the simulation methodology should be validated of the fuel cell simulated in Comsol MultiPhysics. In this work, PEMFC and DMFC fuel cell models have been simulated and validated by experimental data. It means that these two models were validated and can be work in real life. If these two fuel cell models were not validated, the developer has to go back to early stage whereby specifying constants, domain equations and boundary conditions over again.

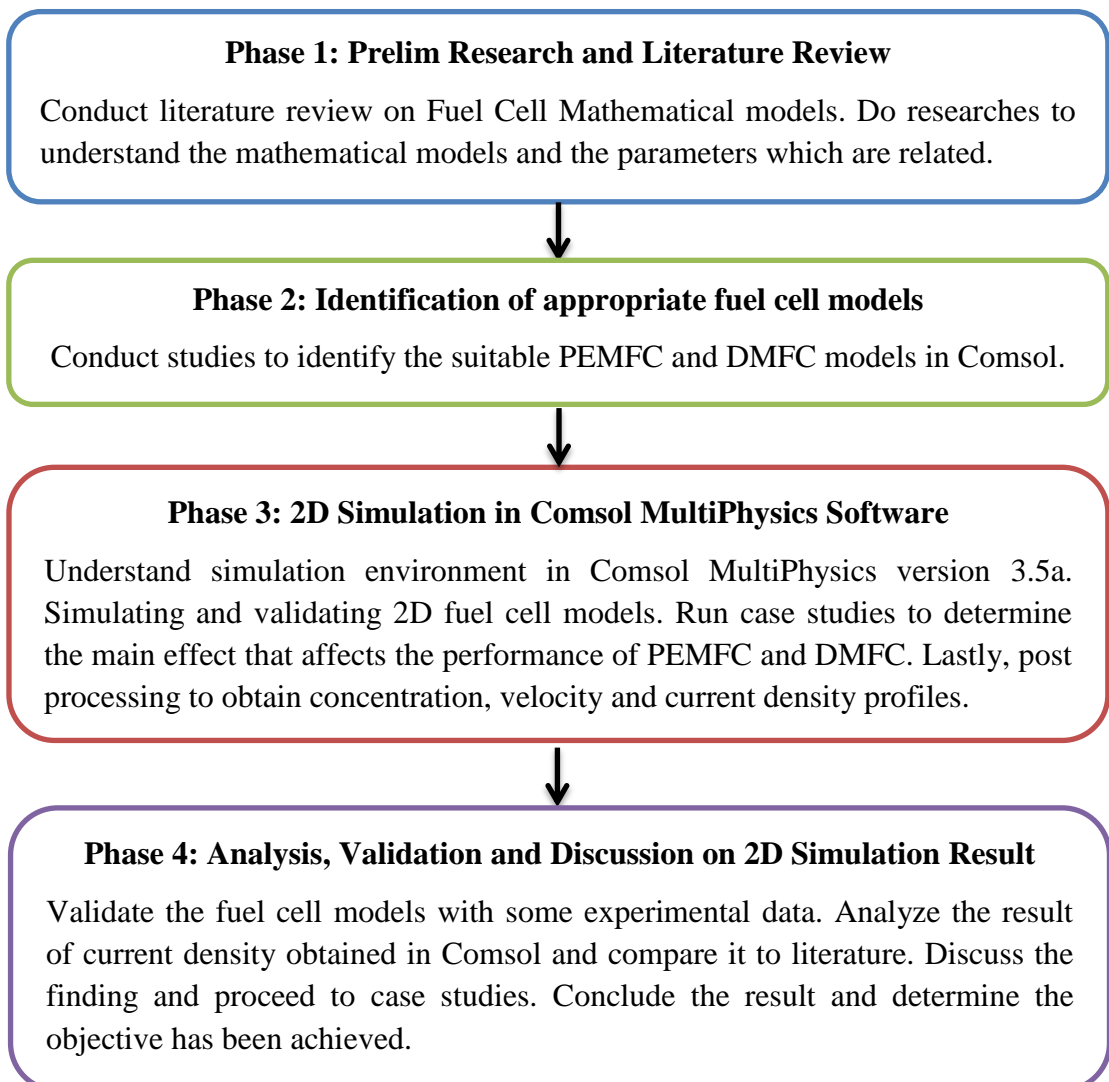
If the fuel cells have been validated, the next step is to run some case studies by manipulating process variables and design variable on fuel cells. As discussed earlier on, those variables which were being investigated in this work were fuel concentration in anode, oxidant concentration in the cathode, directional flow of reactants and different membrane properties by using Taguchi's method. The effects of these variables have been studied and the main effect that affects the performance of a fuel cell has been determined. At the end of this project, the performance of PEMFC and DMFC has been compared in term of power and current density in graphical method in Chapter 4.

3.2 Research Methodology Method

The research methodologies used in design of experiments were Taguchi's Method. Taguchi Method is an orthogonal array which developed by Genichi Taguchi to improve the quality of designing the experiment. A well planned set of experiments, in which all parameters of interest have varied over a specified range, is a much better approach to obtain systematic data. Usually the number of experiments and resources (materials and time) required are prohibitively large if dealing with many variables. By performing the Taguchi's method, a number of experiments can be reduced significantly hence it helps to save time and resources.

3.3 Project Work

Project activities as shown in the following will be performed in each phase of the 2D Simulation Methodology:



3.4 Design of Experiments by using Taguchi Method

There are four parameters need to be investigated with two factors. These parameters included fuel concentration at anode, oxidant concentration at cathode, directional flow of reactants and membrane properties. So, L_8 of Taguchi Method has been chosen in this work as indicated in figure 3.4 below. Originally, there are 2^4 which are 16 experiments needed to be carried out for each fuel cell but by using Taguchi's Method; the number of experiments for each fuel cell is 8. So the amount of experiment can be reduced to half, therefore it save time and resource at all.

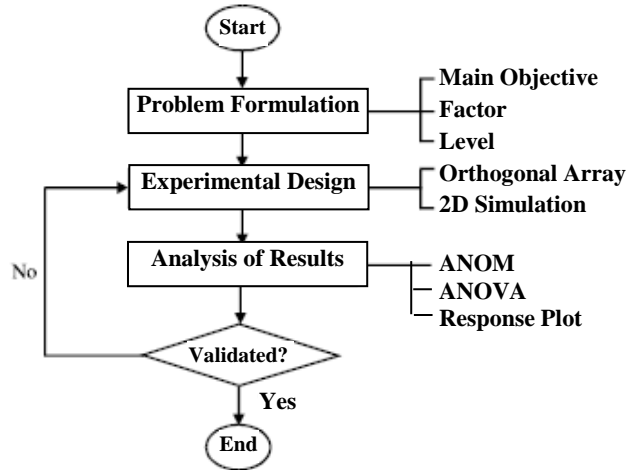


Figure 3.4: Flow Diagram of Taguchi Method

Implementation of Taguchi Method can be illustrated as shown in figure 3.4 above. At the top of that is the formulation of a problem which requires defining a main objective. In this work, the main objective is to maximize the performance of PEMFC and DMFC by using Taguchi Method. Besides that, it also consists of factors and levels of experiment after having an objective function. Controllable factor A to D are set up in an L_8 (2^4). Outputs from running this simulation are the current density of fuel cells.

Next step is to design of experiments which consist of orthogonal array and running simulation of Fuel cells. In this work, there are 4 controllable factors at 2 levels. A L_8 array which consists of 8 rows and 4 columns is appropriate. At this point of view, row is representing simulation run and column represent number of factors in this work. It should be noted that in order to take enough response of all 4 variables toward object function, only 8 simulations run needed to be done for each fuel cell. Design of experiments by using Taguchi's Method showed in Table 3.1 below.

Step 3 is dealing with gather and analysis of results of Simulation. In this work, there are three statistical tools has been used which are ANOM, ANOVA and Response Plot. ANOM is an analysis of mean which is a method to compare means and variances across several groups of result data while Analysis of Variance, ANOVA is a particular form of statistical hypothesis testing heavily used in the analysis of experimental data. A statistical hypothesis test is a method of making decisions using data.

Finally, step four is validation of experimental result. For each run in L8 orthogonal array, it will yield the highest current density of the particular fuel cell. Preliminary visualization of trend of each factor average contribution at all 2 levels can be made through response plot. Response plot is used to identify the optimal design configuration for validating the result obtained from simulation. The equation below is used to calculate the optimum current density by summing up all global mean of current density of a particular fuel cell with maximum deviation of average value of 4 factors with 2 levels.

Table 3.1: L₈ Taguchi Method in 2D Fuel Cell Simulation

	Factors			
Experiment	A	B	C	D
1	1	1	1	1
2	1	1	2	2
3	1	2	2	1
4	1	2	1	2
5	2	1	2	1
6	2	1	1	2
7	2	2	1	1
8	2	2	2	2

3.5 Constants and Parameters Involved in 2D Simulation

3.5.1 Operating Parameters for PEMFC

Table 3.2: Constants Used in 2D PEMFC Model Simulation

Input Parameter	Value
Width of the anode and cathode Channel	$2.5 \times 10^{-4} \text{ m}$
Height of the Electrode	$2 \times 10^{-3} \text{ m}$
Membrane Thickness	$1 \times 10^{-4} \text{ m}$
Collector Height	$1 \times 10^{-3} \text{ m}$
Conductivity of solid phase	1000 S.m^{-1}
Conductivity of membrane	9 S m^{-1}
Cell voltage	0.7V
Gas constant	$8.314 \text{ J.mol}^{-1} \cdot \text{K}^{-1}$
Temperature of Fuel Cell	353 K
Faraday's constant	96485 C.mol^{-1}
Permeability of electrode	$1 \times 10^{-13} \text{ m}^2$
Fluid viscosity	$2.1 \times 10^{-5} \text{ Pa.s}$
Reference atmospheric pressure	$1.013 \times 10^5 \text{ Pa}$
Anode inlet pressure	$1.115 \times 10^5 \text{ Pa}$
Cathode inlet pressure	$1.115 \times 10^5 \text{ Pa}$
Water drag coefficient	3
Equilibrium potential of anode	0 V
Equilibrium potential of cathode	1 V
Exchange current density of anode	$1 \times 10^5 \text{ A.m}^{-2}$
Exchange current density of cathode	1 A m^{-2}
Specific surface area	$1 \times 10^7 \text{ m}^{-1}$
Aggregate radius	$1 \times 10^{-7} \text{ m}$
Active-layer length	$1 \times 10^{-5} \text{ m}$
Porosity of anode and cathode catalyst layer	0.2
Porosity of membrane	0.4
Gas diffusivity in agglomerate model	$4.988 \times 10^{-12} \text{ m}^2 \cdot \text{s}^{-1}$
Effective binary diffusivity of hydrogen in water	$2.85 \times 10^{-5} \text{ m}^2 \cdot \text{s}^{-1}$
Effective binary diffusivity of oxygen in water	$5.81 \times 10^{-6} \text{ m}^2 \cdot \text{s}^{-1}$
Effective binary diffusivity of oxygen in nitrogen	$7.35 \times 10^{-6} \text{ m}^2 \cdot \text{s}^{-1}$
Effective binary diffusivity of hydrogen in nitrogen	$7.97 \times 10^{-6} \text{ m}^2 \cdot \text{s}^{-1}$
Inlet weight fraction, H2	0.1
Inlet weight fraction, O2	0.21*0.8
Cathode inlet weight fraction, H2O	0.2
Henry's law constant, H2 in agglomerate	$3.9 \times 10^4 \text{ Pa.m}^3 \cdot \text{mol}^{-1}$
Henry's law constant, O2 in agglomerate	$3.2 \times 10^4 \text{ Pa.m}^3 \cdot \text{mol}^{-1}$
Reference concentration, H2	1.3 mol.m^{-3}
Reference concentration, O2	0.43 mol.m^{-3}

3.5.2 Operating Parameters for DMFC

Table 3.3: Constants Used in 2D DMFC Model Simulation

Input Parameter	Value
Width of the anode and cathode Channel	$2.5 \times 10^{-4} \text{ m}$
Height of the Electrode	$2 \times 10^{-3} \text{ m}$
Membrane Thickness	$1 \times 10^{-4} \text{ m}$
Collector Height	$1 \times 10^{-3} \text{ m}$
Conductivity of solid phase	1000 S m^{-1}
Conductivity of membrane	14.615 S.m^{-1}
Cell voltage	0.7V
Gas constant	$8.314 \text{ J.mol}^{-1} \cdot \text{K}^{-1}$
Temperature of Fuel Cell	353 K
Faraday's constant	96485 C.mol^{-1}
Permeability of electrode	$1 \times 10^{-13} \text{ m}^2$
Fluid viscosity	$2.1 \times 10^{-5} \text{ Pa.s}$
Reference atmospheric pressure	$1.013 \times 10^5 \text{ Pa}$
Anode inlet pressure	$1.115 \times 10^5 \text{ Pa}$
Cathode inlet pressure	$1.115 \times 10^5 \text{ Pa}$
Water drag coefficient	2.11
Equilibrium potential of anode	0 V
Equilibrium potential of cathode	1 V
Exchange current density of anode	$1 \times 10^5 \text{ A.m}^{-2}$
Exchange current density of cathode	1 A.m^{-2}
Specific surface area	$1 \times 10^7 \text{ m}^{-1}$
Aggregate radius	$1 \times 10^{-7} \text{ m}$
Active-layer length	$1 \times 10^{-5} \text{ m}$
Porosity of anode and cathode catalyst layer	0.28
Porosity of membrane	0.4
Gas diffusivity in agglomerate model	$8.26314 \times 10^{-12} \text{ m}^2 \cdot \text{s}^{-1}$
Effective binary diffusivity of hydrogen in Methanol	$6.8 \times 10^{-5} \text{ m}^2 \cdot \text{s}^{-1}$
Effective binary diffusivity of oxygen in water	$5.81 \times 10^{-6} \text{ m}^2 \cdot \text{s}^{-1}$
Effective binary diffusivity of oxygen in nitrogen	$7.35 \times 10^{-6} \text{ m}^2 \cdot \text{s}^{-1}$
Effective binary diffusivity of hydrogen in nitrogen	$7.97 \times 10^{-6} \text{ m}^2 \cdot \text{s}^{-1}$
Inlet weight fraction, H2	0.11125
Inlet weight fraction, O2	0.21*0.8
Cathode inlet weight fraction, H2O	0.2
Henry's law constant, H2 in agglomerate	$3.9 \times 10^4 \text{ Pa.m}^3 \cdot \text{mol}^{-1}$
Henry's law constant, O2 in agglomerate	$3.2 \times 10^4 \text{ Pa.m}^3 \cdot \text{mol}^{-1}$
Reference concentration, H2	1.3 mol.m^{-3}
Reference concentration, O2	0.43 mol.m^{-3}
Diffusion coefficient of methanol in membrane	$4.9 \times 10^{-9} \text{ m}^2 \cdot \text{s}^{-1}$
Diffusion coefficient of methanol in water	$2.8 \times 10^{-9} \text{ m}^2 \cdot \text{s}^{-1}$
Concentration of Methanol	1M

3.6 Experimental Tools and Software

3.6.1 Fuel Cell Car Toolkit

- It is designed for a "hands on" experience with solar hydrogen energy technology. The solar module converts radiant energy into electrical energy to power the electrolyzer. The electrolyzer breaks water into its basic constituents of hydrogen and oxygen. PEM fuel cell combines the gases to form water, and release heat and electricity.

3.6.2 Comsol MultiPhysics Engineering Simulation Software

- COMSOL Multiphysics is a finite element analysis, solver and simulation software / FEA package for various physics and engineering applications. COMSOL Multiphysics also offers an extensive interface to MATLAB and its toolboxes for a large variety of programming, preprocessing and post processing possibilities.



Figure 3.5: Direct Methanol and Proton Exchange Membrane Fuel Cells

3.7 Key Milestone

The feasibility study will be carried out as well as to identify the constants and domain equations in this work. This is to enable the author to gather the information regarding the fuel cell models and focus on 2D simulation, validation and running case studies and post processing to obtain concentration, velocity and current density profiles.

NO	DETAIL WEEK	1	2	3	4	5	6	7	8	9	10	11	12	13	14
1	Running fuel cell car experiment	★													
2	Simulation 2D DMFC Model		★												
3	Simulation result analysis, discussion and conclusion							★							
4	Validating simulation result and running case studies								★						
5	FYP report writing & presentation														★

★ Suggested Milestone

■ Process

Figure 3.6: Key Milestone

3.8 Gantt Chart

3.8.1 Gantt Chart for Final Year Project I

NO	DETAIL WEEK	1	2	3	4	5	6	7		8	9	10	11	12	13	14
1	Selection of Project Title	■	■													
2	Preliminary Research Work and Literature Review		■	■	■	■										
3	Submission of Extended Proposal Defence						●									
4	Preparation for Oral Proposal Defence							■								
5	Oral Proposal Defence Presentation									■	■					
6	Detailed Literature Review									■	■	■	■	■		
7	Preparation of Interim Report			■	■	■	■	■		■	■	■	■	■		
8	Submission of Interim Draft Report														●	
9	Submission of Interim Final Report															●

● Suggested Milestone

■ Process

Figure 3.7: Gantt Chart for Final Year Project I

3.8.2 Gantt Chart for Final Year Project II

No	Task Name	Week													
		1	2	3	4	5	6	7	8	9	10	11	12	13	14
1	Continue Research Methodology and literature review	■	■	■	■	■	■	■							
2	Analysis of Data and Present Findings			■	■	■	■	■							
3	Identify boundary condition and equation to be evaluated in 2D Fuel Cells models simulation in Comsol MultiPhysics			■	■	■	■								
4	Determine the process variable and design parameter in 2D simulation				■	■									
5	Design the structure of fuel cells				■	■	■	■	■						
6	Submission of Progress Report							■							
7	2D fuel cells models simulation, validation and running case study on Fuel Cells								■	■	■				
8	Preparation of Pre-EDX								■	■	■				
9	Pre-EDX											■			
10	Preparation & Submission of Dissertation												■	■	
11	Viva														■
12	Preparation of Technical Paper												■	■	■
13	Preparation of Final Dissertation												■	■	■
14	Submission of Final Dissertation and Technical Paper														■

Figure 3.8: Timeline for Final Year Project II

CHAPTER 4

RESULT AND DISCUSSION

Before the 2D fuel cell models were designed and simulated, all the information about constants, domain equations, governing equations and boundary condition in the fuel cell system needs to be gathered. Generating mesh and simulating 2D fuel cell model by solving boundary condition problem. After fuel cell simulation, it has been validated via experimental result. Next, running some case studies and manipulating some variables to investigate the main effect of PEMFC and DMFC by using Taguchi Method. Finally, compare the performance in term of Current Density and Power Density of PEMFC and DMFC.

4.1 Validation of 2D Simulated Fuel Cell Models

The result of the 2D DMFC and PEMFC models simulated were compared to the experimental data previously done by some researchers. The dimensions of the cell and operating parameters were given in Table 3.1 (PEMFC) and Table 3.2 (DMFC).

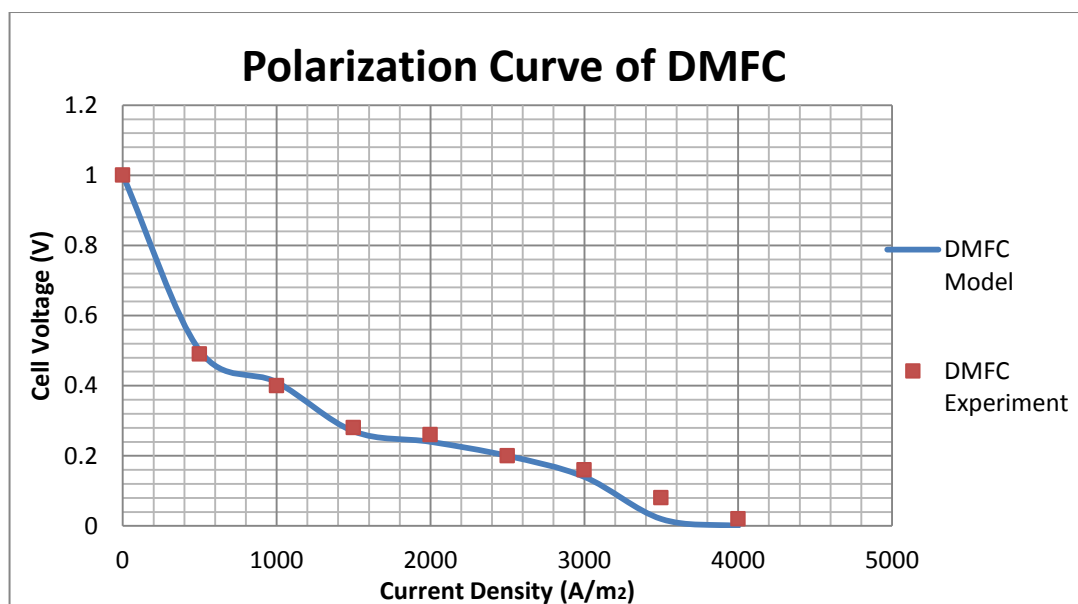


Figure 4.1: Polarization Curve of DMFC

Comparison of the experimental data and the results from simulated DMFC model between the cell voltages of 0 V and 1 V were shown in Fig. 4.1. At high current densities such as 3000 A.m^{-2} , the experimental results show a deviation due to the diffusion limitations. However deviation occurs at higher current densities (higher than 3000 A.m^{-2}) for the model developed. Modeling results show a linear trend for the high current density conditions. It is because of neglecting the two-phase effects in the model developed which has a significant effect on the limiting current density.

For 2D simulated PEMFC, when the operating temperature is decreased, the current density will increase [13]. The same observation was obtained in the PEMFC 2D simulated model. The temperature profile as shown in figure 4.2 is a comparison between experimental data with the simulated PEMFC. It is because temperature and density shares an inverse relationship. As temperature increases, the distance between water molecules (known as density) will be decreased. If density of water decreases, the content of hydrogen molecule also will decrease in a unit area. The concentration of hydrogen in water affects the current density produced by PEMFC. Higher content of hydrogen will generate higher current density in PEMFC [12].

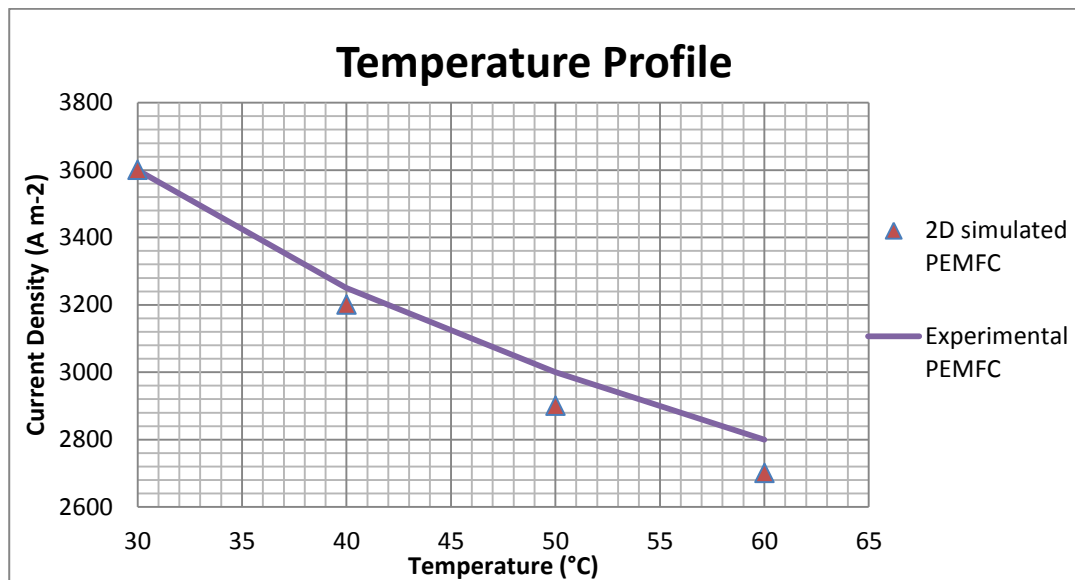


Figure 4.2: Temperature Profile for PEMFC

4.2 Post Processing and Visualization

After simulating 2D fuel cell models by solving boundary condition problems in Comsol as discussed in Chapter 3, concentration, velocity and current density profile has been simulated and post processed as shown in figure 4.3 below.

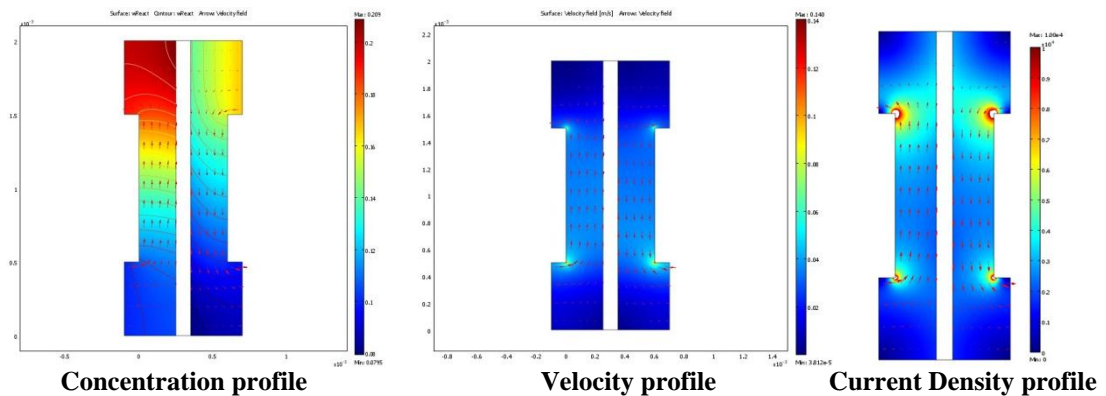


Figure 4.3: Concentration, Velocity and Current Density Profiles

4.2.1 Concentration Profile

The concentration profile in Figure 4.3 above was the reactant (oxygen and hydrogen) weight fractions in the cathode and anode gases. Hydrogen mass fraction increases as the anode gas flows from the inlet (bottom left) to the outlet (top right). This is the result of the osmotic drag coefficient of water through the membrane, which results in a higher flux than the consumption of hydrogen in anode catalyst layer. Therefore the convective flux of anode gas towards the membrane causes the weight fraction of hydrogen to go up. In the cathode gas, there is an expected decrease in oxygen content along the flow direction. It is because oxygen was being consumed to react with hydrogen to form water molecule.

4.2.2 Velocity Profile

The current density is uneven with the highest density in the fuel cell's top region. Oxygen-reduction reaction rate in cathode determines the current-density distribution. The maximum current density arises close to the air inlet.

4.2.3 Current Density Profile

There are significant current spikes present at the corners of the current collectors. For PEMFC, the maximum current density produced is 3600A.m^{-2} while DMFC is 3025A.m^{-2} .

4.3 Data Gathering and Analysis for Fuel Cells

4.3.1 Taguchi Table

Experiment	A	B	C	D	PEMFC		DMFC	
					Current Density (A/m ²)	Power Density (W/m ²)	Current Density (A/m ²)	Power Density (W/m ²)
1	1	1	1	1	2800	1960	1263	884
2	1	1	2	2	3420	2394	1650	1150
3	1	2	2	1	3430	2401	1271	890
4	1	2	1	2	3325	2376	1635	1145
5	2	1	2	1	2636	1845	2300	1610
6	2	1	1	2	3036	2125	2750	1925
7	2	2	1	1	3050	2135	2360	1652
8	2	2	2	2	3600	2520	3025	2117.5

Maximum

LEGEND

A 1 \rightarrow H_2O / $0.5M C_{CH_3OH}$ **B** 1 \rightarrow Air
 2 \rightarrow H_2 / $1M C_{CH_3OH}$ 2 \rightarrow O_2

C 1 \rightarrow Concurrent **D** 1 \rightarrow 117
 2 \rightarrow Counter Current 2 \rightarrow 211

Fuel Concentration **Oxidant** **Flow Direction** **Nafion® Membrane**

Figure 4.4: Result summarizes in Taguchi Method

From figure 4.4 above, it shows that Taguchi Chart that filled with the result of this 2D simulation result. There are four different operating conditions for both fuel cells which are A (fuel concentration in anode channel), B (oxidant concentration in cathode channel), C (directional flow of reactants) and D (different membrane types). Detailed results of all simulations result discussed in Appendix A1 and A2.

Both fuel cells will yield the maximum current density when in higher hydrogen fuel and higher oxidant concentration conditions together with a counter current flow of reactants and using Nafion membrane 211. The maximum current density of the PEMFC is $3600A/m^2$ and DMFC is $3025A/m^2$. The current density different, ΔJ_e between these two fuel cells is $575A/m^2$.

4.3.2 Analysis of Means (ANOM)

The analysis of means (ANOM) is a graphical method for comparing a collection data of means to determine if any one of the data differs significantly from the overall mean. ANOM is a type of multiple comparison method. The results of the analysis are summarized in an ANOM chart. Chart as shown as in figure 4.5 is similar to a control chart. It has a centerline, located at the overall mean of current density, $A.m^{-2}$. Groups of data are plotted on this chart and if one falls beyond centerline, it is statistically different from the overall mean.

Analysis of mean for PEMFC

Table 4.1: ANOM Table for PEMFC

Level	A	B	C	D
1	3080.5000	2973.0000	3052.7500	2979.0000
2	3243.7500	3351.2500	3271.5000	3345.2500
Mean	3162.13	3162.13	3162.13	3162.13
Effect	163.25	378.25	218.75	366.25
Rank	4	1	3	2

Analysis of mean for DMFC

Table 4.2: ANOM Table for DMFC

Level	A	B	C	D
1	1454.7500	1990.7500	2002.0000	1798.5000
2	2608.7500	2072.7500	2061.5000	2265.0000
Mean	2031.75	2031.75	2031.75	2031.75
Effect	1154.00	82.00	59.50	466.50
Rank	1	3	4	2

(*Note: All results in the tables above are in term of current density, A. m⁻²)

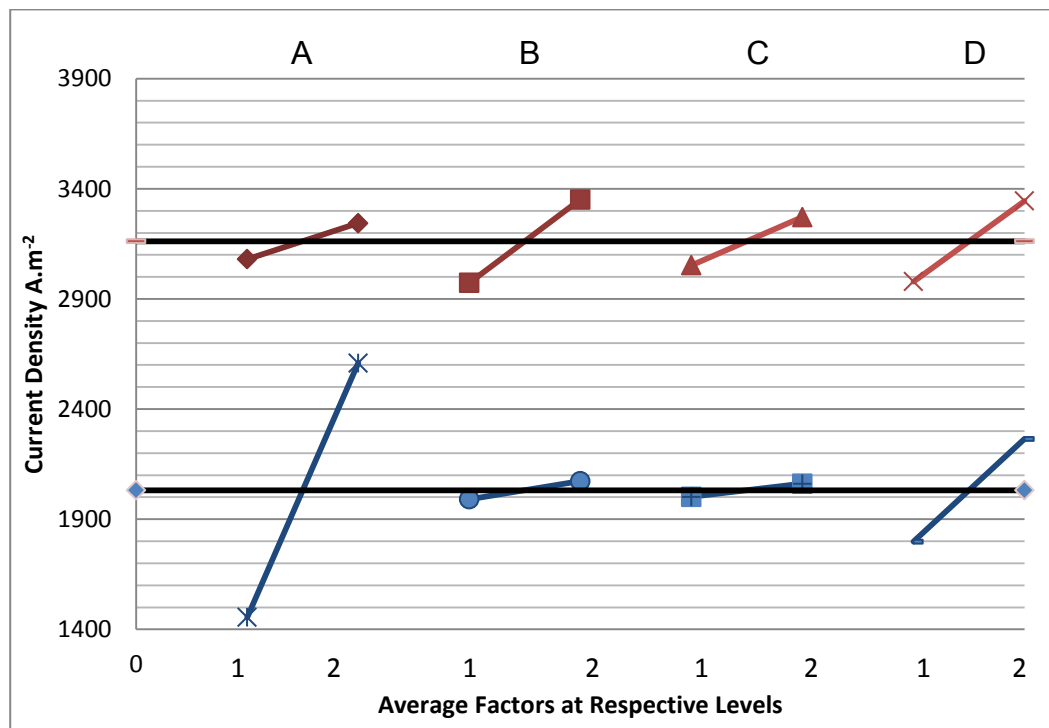


Figure 4.5: ANOM Plot

Figure 4.5 shown above is ANOM Plot whereby red line represents PEMFC and the blue line represents DMFC. From table 4.1 and figure 4.5, factor B (Oxidant concentration) affect the most in PEMFC performance. While factor A (Methanol Concentration) gives the most impact on DMFC performance. From

ANOM plot, A₂B₂C₂D₂ is the best configuration for PEMFC and DMFC. It gives the maximum current density for these both fuel cells. Higher fuel and oxidant concentration accelerate the chemical redox reaction in fuel cells, counter current flow of reactants maximizes the transfer rate of heat and mass and finally by using Nafion® 211membrane, there is more hydrogen ion can pass through membrane to combine with oxygen to form water and produce electricity.

4.3.3 Analysis of Variance (ANOVA)

In statistics, **Analysis of Variance (ANOVA)** is a collection of statistical data, and their associated method, in which the variance in a particular manipulated variable is separated into components attributable to different variation. ANOVA provides a statistical test of whether or not the means of several groups are all equal. Furthermore, ANOVAs are useful in comparing two, three, or more means. The terminology of ANOVA is largely from the statistical design of experiments. Factors are assigned to experimental units by a combination of randomization and blocking to ensure the validity of the results by using Taguchi orthogonal array.

Table 4.3: ANOVA for PEMFC

Level	A	B	C	D	
1	6662.64	35768.27	11962.89	33534.77	
2	6662.64	35768.27	11962.89	33534.77	
Sum	13325.28	71536.53	23925.78	67069.53	
Sum of Square	106602.3	572292.3	191406.25	536556.3	
DOF	1	1	1	1	Total
Variance of factor 1	106602.3	572292.3	191406.25	536556.3	1406857
% Contribution	7.577334	40.67878	13.6052385	38.13865	100
Rank	4	1	3	2	

Table 4.4: ANOVA for DMFC

Level	A	B	C	D	
1	332929.00	1681.00	885.06	54405.56	
2	332929.00	1681.00	885.06	54405.56	
Sum	665858.00	3362.00	1770.13	108811.13	
Sum of Square	5326864	26896	14161	870489	
DOF	1	1	1	1	Total
Variance of factor 1	5326864	26896	14161	870489	6238410
% Contribution	85.38817	0.431135	0.226997	13.9537	100
Rank	1	3	4	2	

4.3.4 Main Effect Response Plot

The main Effect plot shows how the mean response of a factor varies over the levels investigated for that factor. Levels of this factor are marked on the x-axis. The mean values of all samples studied at the respective levels are plotted on the y-axis. This plot shows the main effect of factor A, B, C, and D while the mean response is displayed in 2 levels of all 4 factors. The effects plots may also show 'bars' about each plotted point as shown as in the figure 4.6 below. These bars allow for a statistical test for the difference between the mean responses of all levels.

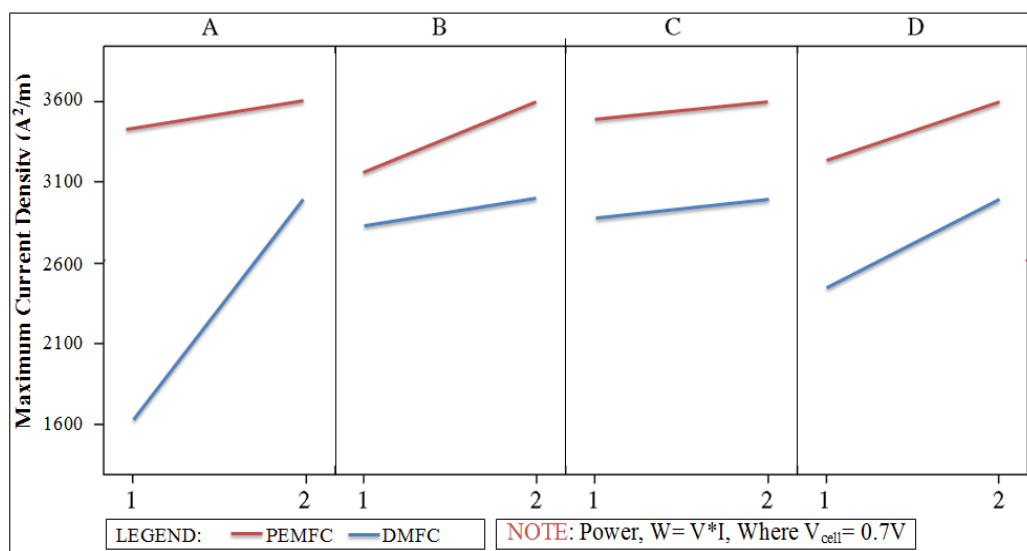


Figure 4.6: Main Response Plot

4.3.4.1 Effect of Fuel Concentration in Anode Channel

From figure 4.6 above, PEMFC generate higher current density from A₂ (pure hydrogen) than A₁ (water) in anode channel. It is because the hydrogen fuel concentration in pure hydrogen gas is higher than in water. There is more hydrogen molecule in anode channel can diffuse through the membrane and react with oxygen in cathode channel to form water molecule and produce higher current density. From the figure shown above, the effect of fuel concentration in anode channel is significantly on fuel cell's performance.

By using 1 Molar or 3wt % of methanol concentration in DMFC's anode, it generates higher current density than in 0.5 Molar of methanol concentration.

From the figure 4.7 below, when the concentration of methanol increased, the current density generated will be increased. It is because there is more hydrogen molecules in anode channel diffuse through the membrane and react with oxygen in the cathode, causing the formation of water molecule and production of higher current density. The effect of fuel concentration in anode channel ranks the first and the most significant effect in DMFC as shown in ANOM Plot and Response Plot.

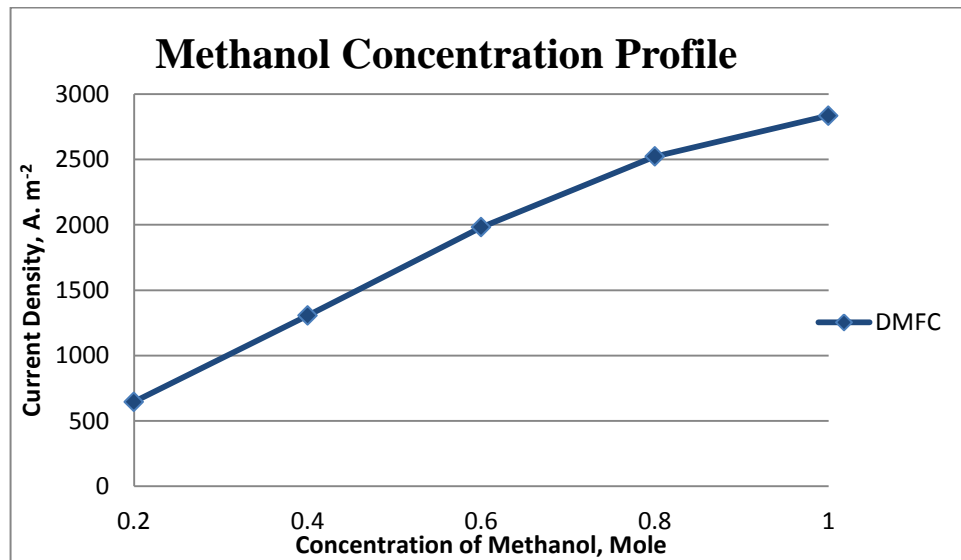


Figure 4.7: Methanol Concentration Profile in DMFC

4.3.4.2 Effect of Oxidant Concentration in Cathode Channel

By using pure oxygen gas, factor B₂ in PEMFC's cathode, current density generated will increase. It is because there is more oxygen can react with hydrogen molecules which travelled from anode channel to form water molecules and produce higher current density. The more oxygen reacts with hydrogen, the higher of the current and power density produced at current collector at the cathode.

By using different concentration of oxygen in cathode in DMFC, current density produced will be affected. When using 100% concentration of oxygen in Cathode, it will produce more current density. Oxygen concentration in air is only 21% while 79% is Nitrogen. If air used as oxidant of factor B₁, current density produced is not that much compared to pure oxygen as shown in figure 4.8 below.

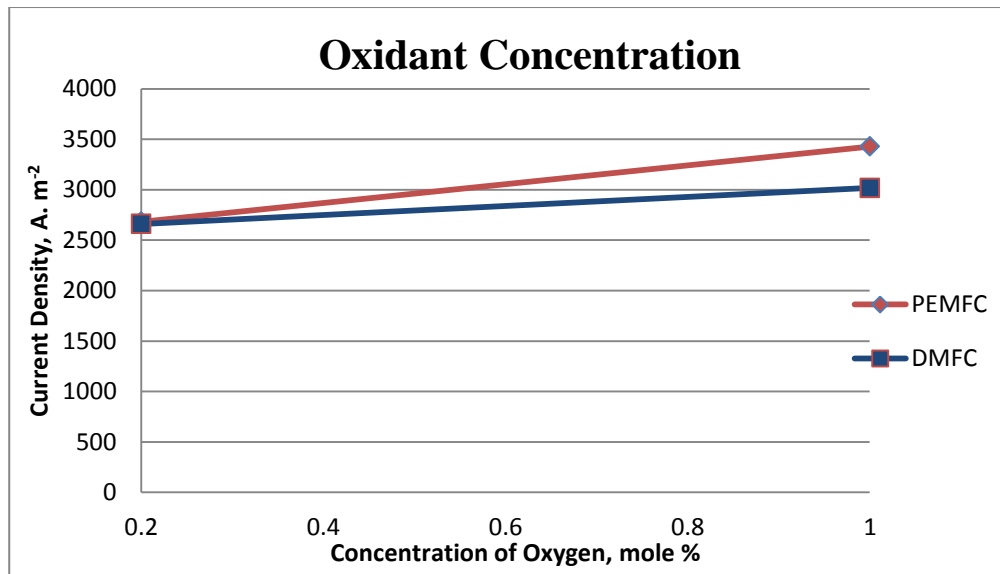


Figure 4.8: Oxygen Concentration in PEMFC and DMFC

4.3.4.3 Effect of Directional Flow of Reactants

Current Density generated in the counter current flow, factor C_2 is higher than in concurrent flow (factor C_1) of reactants in PEMFC. It is because there is more heat and mass transfer rate between flow channel and membrane in counter current flow if comparable to concurrent flow of reactants. Higher mass and heat contact can generate higher current density. Finally, the current density peak generated by the counter current direction flow of reactants is increased and achieves optimum value in PEMFC as shown in figure 4.9 below.

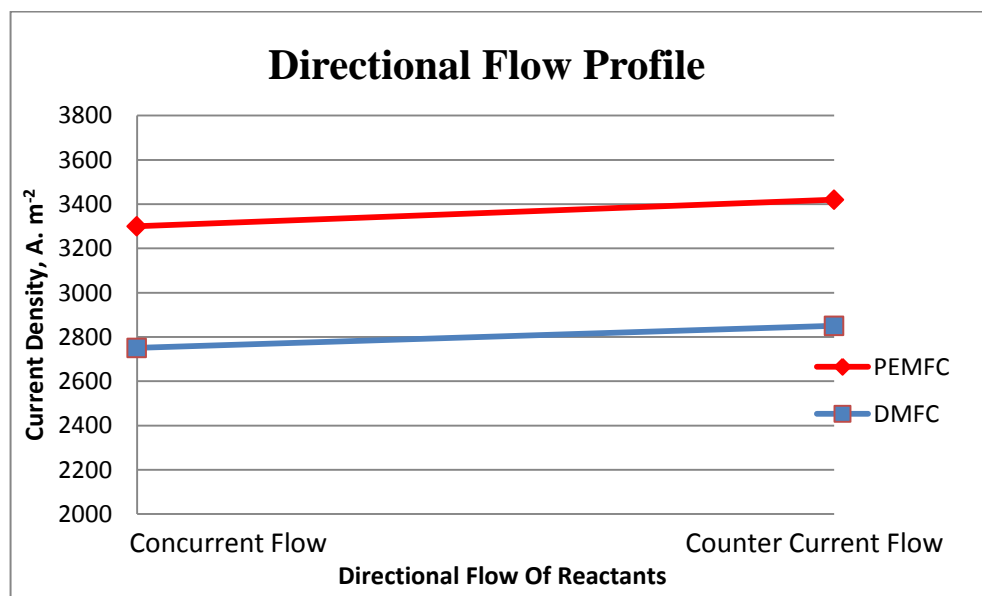


Figure 4.9: Directional Flow Profile in PEMFC and DMFC

The result generated from counter current is higher than in concurrent flow of reactants in DMFC. Methanol enters DMFC at the left top of DMFC and exit at the left bottom. Oxygen enters DMFC at the right bottom and exit at the right top end. This creates a counter current flow of reactants in DMFC and yield maximum performance in term of current and power density.

4.3.4.4 Effect of Different Membrane Properties

Generally there are two commonly used membranes in Fuel cell which are Nafion® 117 and Nafion® 211. From Table 4.5 below, Nafion® 211 has a cheaper price, thicker and lighter properties than Nafion® 117. Besides that, Nafion® 211 is very commonly used in PEMFC due to the channel loading which consist of large amounts of catalyst that will accelerate the current density produced by the fuel cell.

Table 4.5: Comparison between Membranes

Nafion® 117	Specification	Nafion® 211
Non-reinforced film based on chemical stabilized perfluorosulfonic acid /PTFE copolymer in acid form.	Description	Exhibit substantially lower fluoride ion released an improved chemical durability. The polymer is chemical resistant.
Width: 0.3m (Min) - 1.22m (Max) Length: 0.3m (Min) - 1.22m (Max)	Sizing Available	Width: 0.305m (Min) -0.610m (Max) Length: Typically 100m
183	Typical Thickness (Microns)	25.4
360	Basis Weight(g/m²)	50
\$25 100cm²	Pricing (USD \$)	100m ² \$15
Cathode Loading: 0.5 mg/cm ² 60 wt% Pt Anode Loading: 0.5 mg/cm ² 60 wt% Pt	Channel Loading	Cathode Loading: 4mg/cm ² Pt Anode Loading: 4 mg/cm ² Pt:Ru

Porosity for Nafion® 211 is 0.28Micron while porosity for Nafion® 117 is 0.20Micron. In simulation, both Nafion® membranes have to be taken into consideration. In order to build the best model that yields a higher current

density, a comparison has been made between these two Nafion® membranes. Detailed result of the comparison will be shown in figure 4.10.

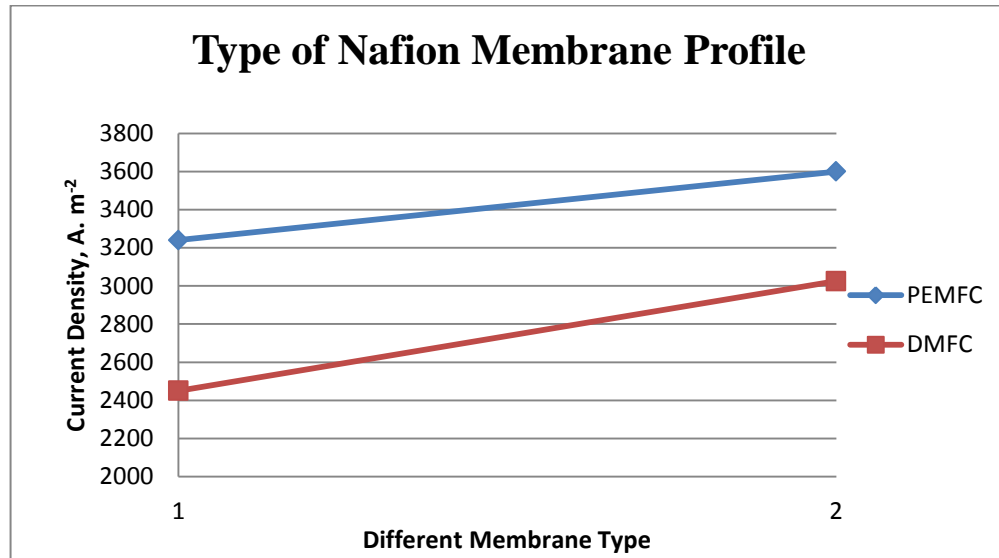


Figure 4.10: Type of Nafion Membrane Profile

Current Density peak generated by Nafion® 211 membrane is higher than Nafion® 117 membranes. This value is very significant if membrane Nafion® 211 used in a fuel cell application. The larger the porosity of a membrane, the better the transfer rate of proton across membrane. When the size of the hole in the membrane is increasing, it will allow more ions to pass by it, therefore there is more hydrogen ion can combine with oxygen ion to produce heat, electricity and water. Finally, the current density peaks generated by using this membrane is increased and achieve optimum value of both fuel cells.

4.4 Validation for Taguchi Method

The last session in Taguchi Method is validation of the Taguchi Chart. For each case study in this project, there are 8 combinations of experimental runs for each fuel cell. By simulation design, only one will yield the highest current density. Preliminary visualization of trends of each factor contributions at all levels is possible through an effect plot. Here, average values of factor k , \bar{x}_{ki} are plotted against all 2 levels in this project. The effect plot may be used to locate optimum design configuration for the purpose of verifying the results. An additional experiment is run to compare both experimental and calculated outputs (current density). The calculated optimum

current density x_{opt} is obtained by summing up global mean \bar{x} with maximum deviations of average of 4 factors over all 2 levels, \bar{x}_{kl} from its corresponding average \bar{x}_k .

$$x_{opt} = \bar{x} + [\sum_{k=1}^k \max(\bar{x}_{kl}) - \bar{x}_k]; \forall l = 1, \dots, L \quad (19)$$

Where, $\bar{x}_k = \bar{x}; \forall k = 1, \dots, K \quad (20)$

For PEMFC

The Optimal current density is 3600 A.m⁻² from A₂B₂C₂D₂ configurations.

Global Mean from all 8 simulations run is 3162.125 A.m⁻²

X_{opt} is calculated based on equation 21.

$$X_{opt} = 3162.125 + (81.625 + 189.125 + 109.375 + 183.125) = \underline{3725.375 \text{ A.m}^{-2}}$$

Table 4.6: Validation Table for PEMFC

Level	A	B	C	D
Maximum	3243.75	3351.25	3271.5	3345.25
Mean	3162.125	3162.125	3162.125	3162.125
Max-Mean	81.625	189.125	109.375	183.125
X _{opt}	3725.375			

% Difference of Optimum Current Density

$$= \frac{3725.375 - 3600}{3600} \times 100\% = 3.48\% (<20\%, \text{Acceptable})$$

For DMFC

The Optimal current density for DMFC is 3025A.m⁻² from A₂B₂C₂D₂ configurations.

Global Mean from all 8 simulations run is 2031.75 A.m⁻²

X_{opt} is calculated based on equation 21.

$$X_{opt} = 2912.75 + (577 + 41 + 29.75 + 233.25) = \underline{2912.75 \text{ A.m}^{-2}}$$

Table 4.7: Validation Table for DMFC

Level	A	B	C	D
Maximum	2608.75	2072.75	2061.5	2265
Mean	2031.75	2031.75	2031.75	2031.75
Max-Mean	577	41	29.75	233.25
X _{opt}	2912.75			

% Difference of Optimum Current Density

$$= \frac{3025 - 2912.75}{3025.75} \times 100\% = 3.71\% (<20\%, \text{Acceptable})$$

For validation purpose, PEMFC and DMFC have been compared with the calculated optimal result of current density. For PEMFC, X_{opt} has been compared with the maximum current density of 2D simulated PEMFC. Percentage difference of these two optimal values is 3.365%. This value is acceptable because the difference between these two is not that much and only approximately $100 \text{ A}\cdot\text{m}^{-2}$. While for DMFC, the percentage difference between calculated optimal current density, X_{opt} with simulated result is only 3.854%. It shows that both PEMFC and DMFC are validated and acceptable by using $A_2B_2C_2D_2$ configuration in Taguchi Method.

4.5 Comparison of PEMFC and DMFC

From figure 4.11 below, it shows that the performance comparison between PEMFC and DMFC in optimum operating conditions which are higher fuel and oxidant concentration, counter current flow of reactants and using Nafion 211 membrane ($A_2B_2C_2D_2$). PEMFC has better performance ($3600 \text{ A}/\text{m}^2$) than DMFC, ($3025 \text{ A}/\text{m}^2$) whereby the current density different, ΔJ_e is $575 \text{ A}/\text{m}^2$. The best justification of this statement is the fraction of hydrogen fuel used in PEMFC is much higher than in DMFC. The more the hydrogen molecules in anode channel, the more the redox reaction will be occurred in the fuel cell to generate electricity at the cathode current collector.

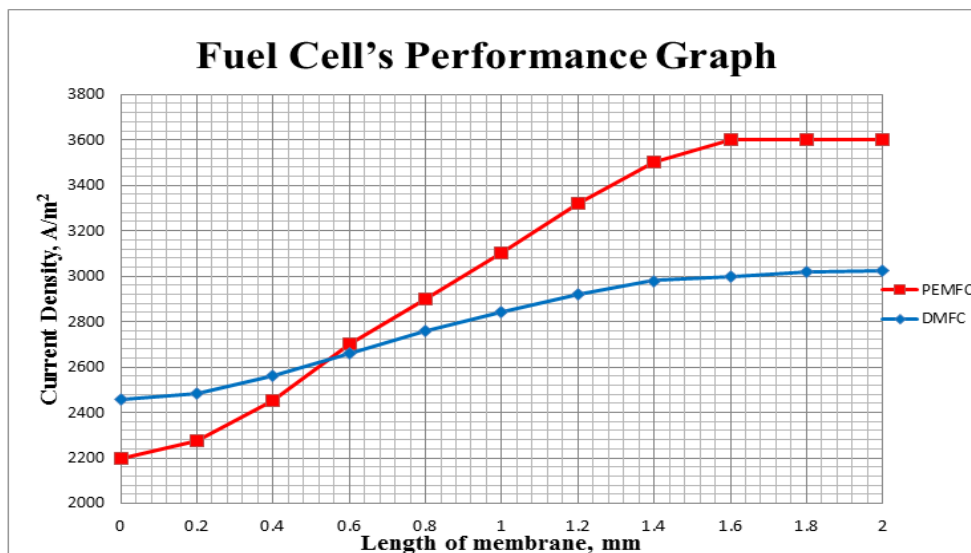


Figure 4.11: Fuel Cell Performance Graph for PEMFC and DMFC

4.6 Concluding Remark

This Design of Experiments (DOE) technique includes the main effect plot and Taguchi's method in this work that enables a developer to determine simultaneously the individual and interactive effects of many factors that could affect the output current density results in any design of a fuel cell. DOE also provides a full insight of interaction between design elements and the operating process variables. Therefore, DOE helps to pinpoint the sensitive parts and sensitive areas in designs that cause problems in Yield/ efficiency problem in fuel cells. A developer can be able to fix them and produce robust and higher yield/ efficient designs.

CHAPTER 5

CONCLUSIONS AND RECOMMENDATIONS

640

5.1 Conclusions

Two-dimensional multi-physics models for PEMFC and DMFC has been developed in Comsol MultiPhysics version 3.5a to simulate the performance of the fuel cells and to investigate the effects of some of the key operating parameters. These models enable us to view in two-dimensional and study the effect of fuel and oxidant concentration, reactants' flow direction and membrane properties over the full range of operating current densities and performance. There is a good agreement between the results of the 2D simulated models with the experimental data in the validation section in Chapter 4. In this study, oxidant concentration in cathode channel has much influence current and power density of PEMFC while fuel concentration in anode channel is the main effect that affects DMFC's performance as shown in figure 5.1 and Table 5.1 below. The best performance in a fuel cell is from $A_2B_2C_2D_2$ arrangement. In conclusion, PEMFC has better performance (max $3600A/m^2$) than DMFC (max $3025A/m^2$) whereby the current density different, ΔJ_e is $575A/m^2$ in optimum operating conditions.

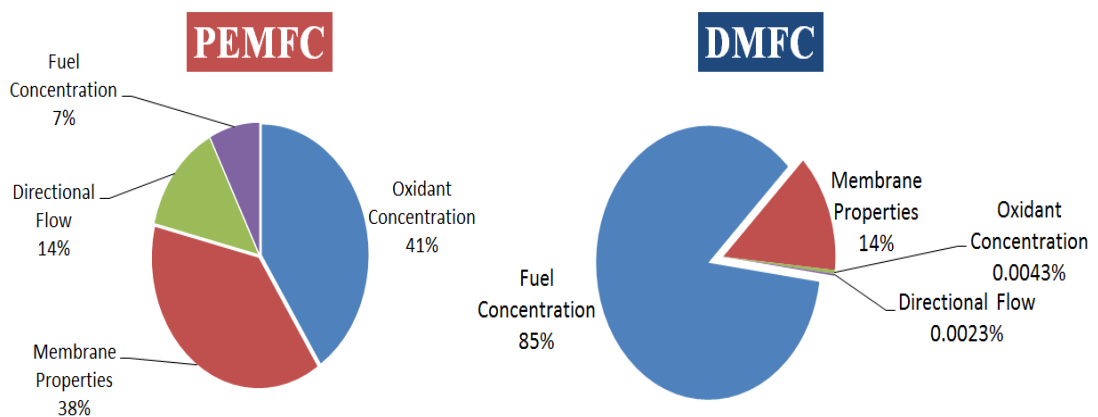


Figure 5.1: Fuel Cell Performance Pie Chart for PEMFC and DMFC

Table 5.1: Conclusion remark for PEMFC and DMFC

	PEMFC		DMFC	
	Simulation	Theory	Simulation	Theory
Optimum Configuration	$A_2B_2C_2D_2$			
Optimum Current Density , A.m⁻²	3600	3725.375	3025	2912.75

5.2 Recommendations

In order to conduct a comprehensive optimization, further work is needed to improve this project such as the inclusion of liquid water/methanol management. Future work might include of study and optimize other parameter as well such as, channel structure and design, reactant velocity/ pressure and so on. Channel structural and design might affect the performance of a fuel cell. Different direction input of reactant will affect the output current density. Yong et al. (2009) explained that gas flow direction in the anode and cathode has a great effect on the performance characteristics of a Fuel Cell. Further improvements in the DMFC model may be realized with an improved anode and a cathode model which allow for the mixed potential at the channel due to methanol crossover problem and porous electrode diffusion in the anode catalyst layer. In order to understand the difference of their performance depending on the flow type, distributions of pressure, temperature and current density were examined and the fractions of various losses were scrutinized.

REFERENCES

1. A. Smirnov, A. Burt, I. Celik, 2006, "Multi-physics simulations of fuel cells using multi-component modeling," *Journal of Power Sources*, **158 (1)**: 295-302.
2. C. K. Dyer, 2002, "Fuel cells for portable applications," *Journal of Power Sources*, **106 (1-2)**: 31-34.
3. C. O. Colpan, A. Funga, F. Hamdullahpur, 2012, "2D modeling of a flowing-electrolyte direct methanol fuel cell," *Journal of Power Sources*, **209**: 301-311.
4. C. Siegel, 2008, "Review of computational heat and mass transfer modeling in polymer-electrolyte-membrane (PEM) fuel cells," *Journal of Energy*, **33 (9)**: 1331-1352.
5. L. Feng, W. Cai, C Li, J. Zhang, C. Liu, W. Xing, 2012, "Fabrication and performance evaluation for a novel small planar passive direct methanol fuel cell stack," *Fuel*, **94**: 401-408.
6. M. M. Hasani-Sadrabadi, E. Dashtimoghadam, F. S. Majedi, K. Kabiri, M. Solati-Hashjin, H. Moaddel, 2010, "Novel nanocomposite proton exchange membranes based on Nafion and AMPS-modified montmorillonite for fuel cell applications," *Journal of Membrane Science*, **365 (1-2)**: 286-293.
7. N. Jung, Y. H. Cho, M. Ahn, J. W. Lim, Y. S. Kang, D. Y. Chung, J. Kim, Y. H. Cho, Y. E. Sung, 2011, "Methanol-tolerant cathode electrode structure composed of heterogeneous composites to overcome methanol crossover effects for direct methanol fuel cell," *International Journal of Hydrogen Energy*, **36 (24)**: 15731-15738.
8. O. Lottin, B. Antoine, T. Colinart, S. Didierjean, G. Maranzana, C. Moyne, J. Ramousse, 2009, "Modelling of the operation of Polymer Exchange Membrane Fuel Cells in the presence of electrodes flooding," *International Journal of Thermal Sciences*, **48 (1)**: 133-145.

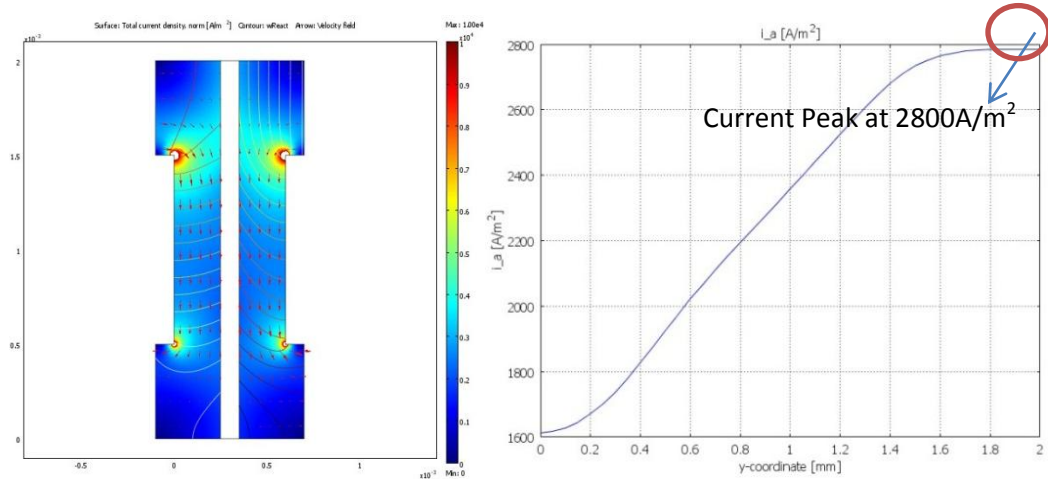
9. S. Basri, S. K. Kamarudin, 2011, "Process system engineering in direct methanol fuel cell," *International Journal of Hydrogen Energy*, **36 (10)**: 6219-6236.
10. S. Bose, T. Kuila, T. X. H. Nguyen, N. H. Kim, K. Lau, J. H. Lee, 2011, "Polymer membranes for high temperature proton exchange membrane fuel cell: Recent advances and challenges," *Progress in Polymer Science*, **36 (6)**: 813-843.
11. S. C. Thomas, X. Ren, S. Gottesfeld, P. Zelenay, 2002, "Direct methanol fuel cells: progress in cell performance and cathode research," *Electrochimica Acta*, **47 (22-23)**: 3741-3748.
12. S. J. Peighambaroust, S. Rowshanzamir, M. Amjadi, 2010, "Review of the proton exchange membranes for fuel cell applications," *International Journal of Hydrogen Energy*, **35 (17)**: 9349-9384.
13. S. K. Kamarudin, F. Achmad, W. R. W. Daud, 2009, "Overview on the application of direct methanol fuel cell (DMFC) for portable electronic devices," *International Journal of Hydrogen Energy*, **34 (16)**: 6902-6916.
14. T. S. Zhao, C. Xu, R. Chen, W. W. Yang, 2009, "Mass transport phenomena in direct methanol fuel cells," *Progress in Energy and Combustion Science*, **35 (3)**: 275-292.
15. V. S. Silva, A. Mendes, L. M. Madeira, S. P. Nunes, 2006, "Proton exchange membranes for direct methanol fuel cells: Properties critical study concerning methanol crossover and proton conductivity," *Journal of Membrane Science*, **276 (1-2)**: 126-134.
16. W. R. Grove, 1842, "On a Gaseous Voltaic Battery," *The London, Edinburgh and Dublin Philosophical Magazine and Journal of Science*, Series 3, **21**: 417-420.
17. Y. Jun, H. Zarrin, M. Fowler, Z. Chen, 2011, "Functionalized titania nanotube composite membranes for high temperature proton exchange membrane fuel cells," *International Journal of Hydrogen Energy*, **36 (10)**: 6073-6081.

APPENDICES

A.1 Data Gathering and Analysis for PEMFC using Taguchi's Method

A.1.1 Experiment 1

Condition: A₁ (H₂O), B₁ (Air), C₁ (Concurrent flow) and D₁ (Nafion® 117)



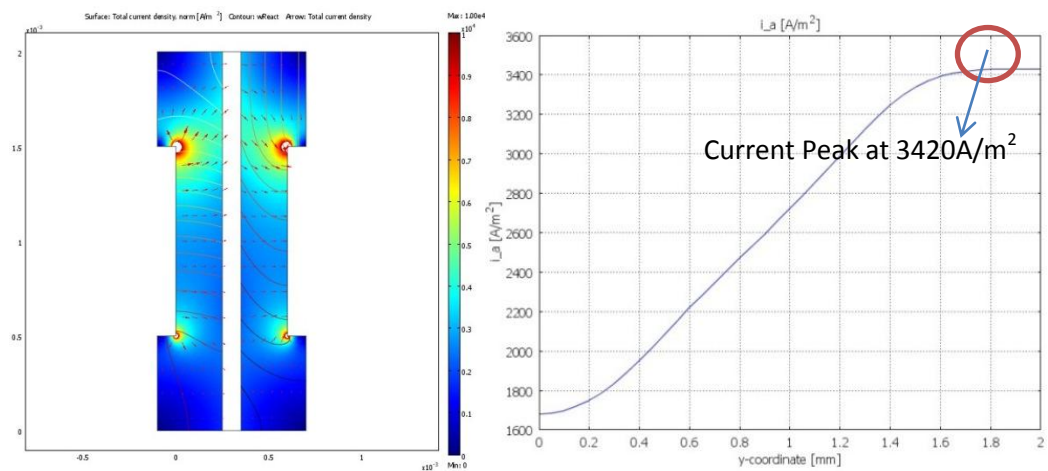
Current density peak generated in experiment 1 is 2800A.m⁻²

Power Density: $W = \text{Current Density} \times \text{Cell's Voltage}$

$$W = 2800\text{A.m}^{-2} * 0.7\text{V} = \underline{\underline{1960\text{W.m}^{-2}}}$$

A.1.2 Experiment 2

Condition: A₁ (H₂O), B₁ (Air), C₂ (Counter current Flow), D₂ (Nafion® 211)



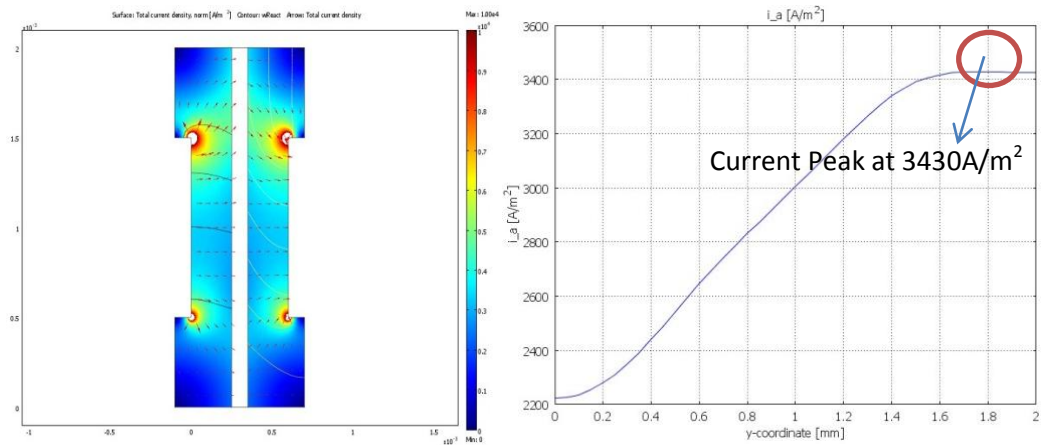
Current density peak generated in experiment 1 is 3420A.m⁻²

Power Density: $W = \text{Current Density} \times \text{Cell's Voltage}$

$$W = 3420\text{A.m}^{-2} * 0.7\text{V} = \underline{\underline{2394\text{W.m}^{-2}}}$$

A.1.3 Experiment 3

Condition: A₁ (H₂O), B₂ (O₂), C₂ (Counter current Flow), D₁ (Nafion® 117)



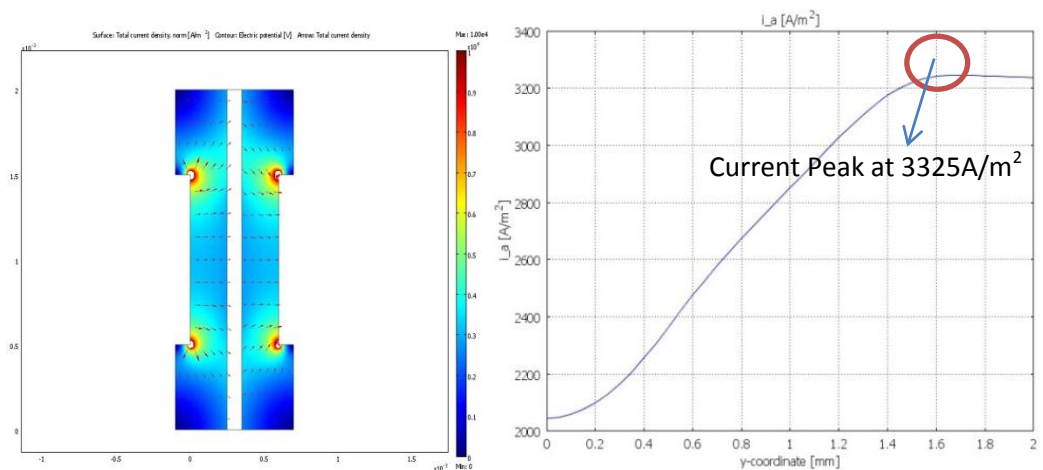
Current density peak generated in experiment 1 is **3430A.m⁻²**

Power Density: $W = \text{Current Density} \times \text{Cell's Voltage}$

$$W = 3430 \text{A.m}^{-2} * 0.7 \text{V} = \underline{\underline{2401 \text{W.m}^{-2}}}$$

A.1.4 Experiment 4

Condition: A₁ (H₂O), B₂ (O₂), C₁ (Concurrent Flow), D₂ (Nafion® 211)



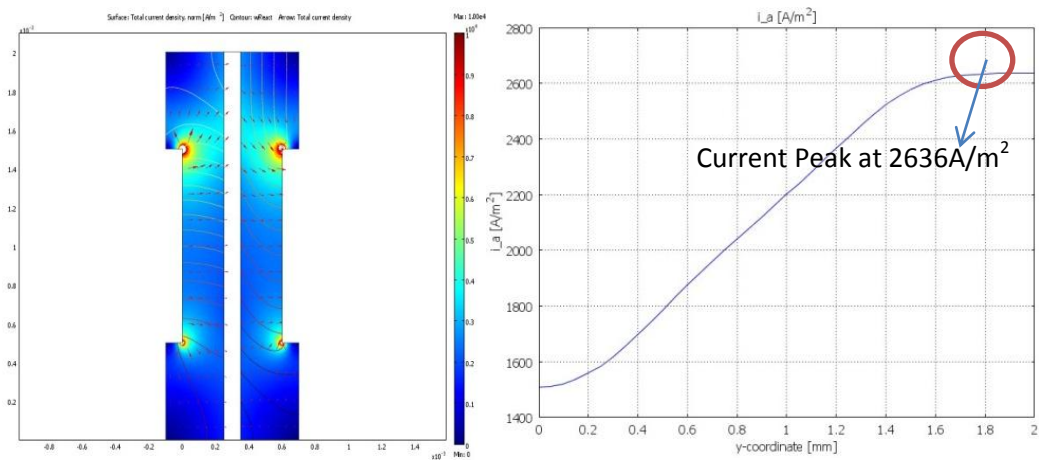
Current density peak generated in experiment 1 is **3325A.m⁻²**

Power Density: $W = \text{Current Density} \times \text{Cell's Voltage}$

$$W = 3325 \text{A.m}^{-2} * 0.7 \text{V} = \underline{\underline{2376 \text{W.m}^{-2}}}$$

A.1.5 Experiment 5

Condition: A₂ (H₂), B₁ (Air), C₂ (Counter current Flow), D₁ (Nafion® 117)



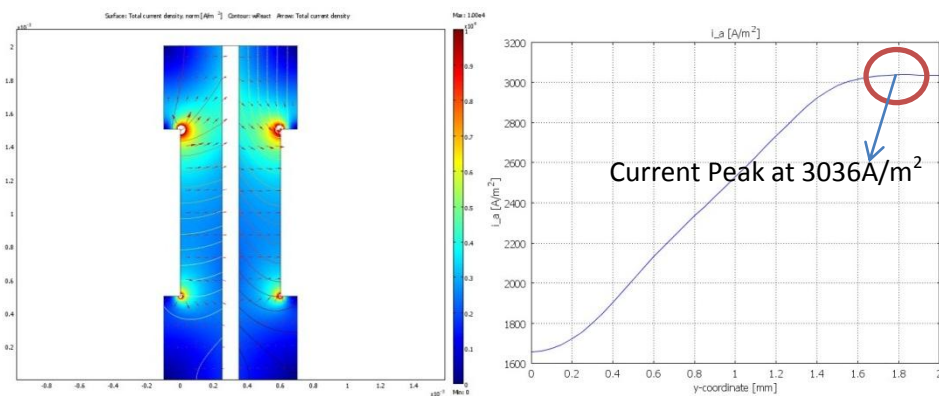
Current density peak generated in experiment 1 is 2636A.m⁻²

Power Density: W= Current Density x Cell's Voltage

$$W = 2636 \text{A.m}^{-2} * 0.7 \text{V} = \underline{\underline{1845 \text{W.m}^{-2}}}$$

A.1.6 Experiment 6

Condition: A₂ (H₂), B₁ (Air), C₁ (Concurrent Flow), D₂ (Nafion® 211)



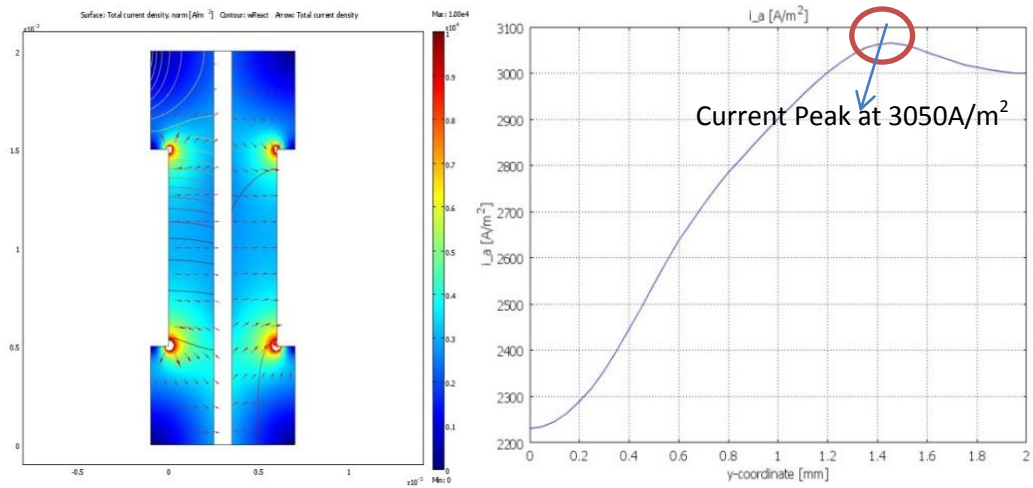
Current density peak generated in experiment 1 is 3036A.m⁻²

Power Density: W= Current Density x Cell's Voltage

$$W = 3036 \text{A.m}^{-2} * 0.7 \text{V} = \underline{\underline{2125 \text{W.m}^{-2}}}$$

A.1.7 Experiment 7

Condition: A₂ (H₂), B₂ (O₂), C₁ (Concurrent Flow), D₁ (Nafion® 117)



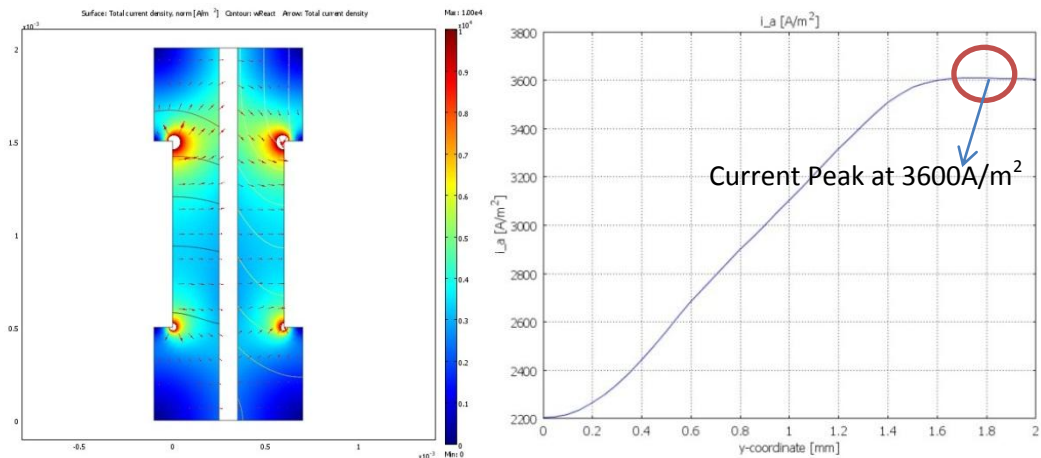
Current density peak generated in experiment 1 is **3050A.m⁻²**

Power Density: W= Current Density x Cell's Voltage

$$W = 3050\text{A.m}^{-2} * 0.7\text{V} = \underline{\underline{2135\text{W.m}^{-2}}}$$

A.1.8 Experiment 8

Condition: A₂ (H₂), B₂ (O₂), C₂ (Counter current Flow), D₂ (Nafion® 211)



Current density peak generated in experiment 1 is **3600A.m⁻²**

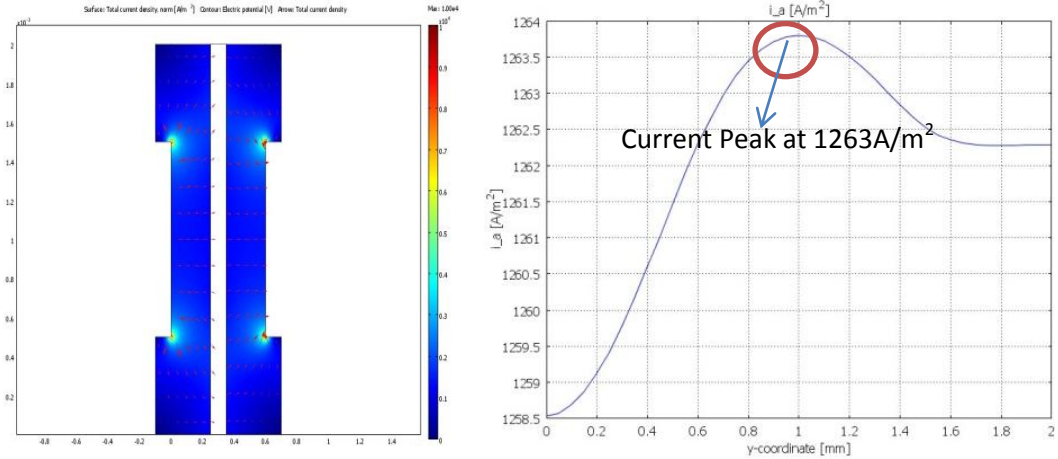
Power Density: W= Current Density x Cell's Voltage

$$W = 3600\text{A.m}^{-2} * 0.7\text{V} = \underline{\underline{2520\text{W.m}^{-2}}}$$

A.2 Data Gathering and Analysis DMFC using Taguchi's Method

A.2.1 Experiment 1

Condition: A₁ (0.5M CH₃OH), B₁ (Air), C₁ (Concurrent), D₁ (Nafion® 117)



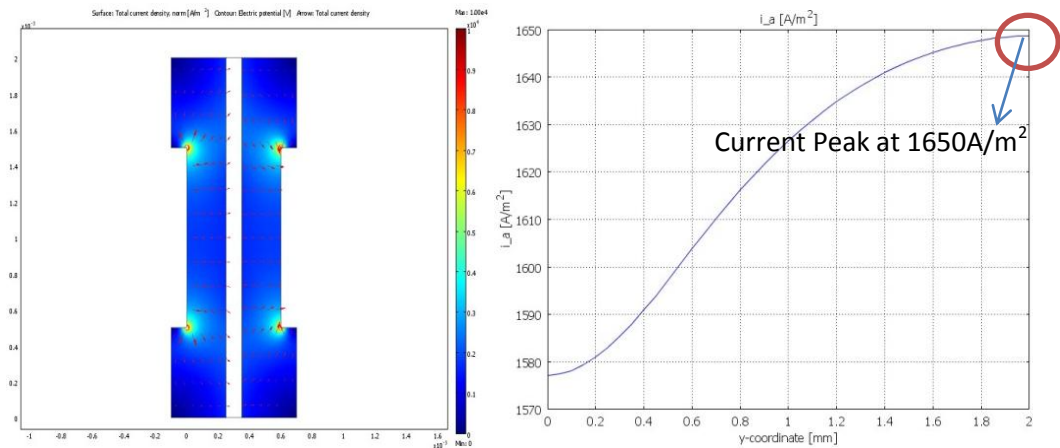
Current density peak generated in DMFC's experiment 1 is 1263A.m⁻²

Power Density: W= Current Density x Cell's Voltage

$$W = 1263 \text{A.m}^{-2} * 0.7 \text{V} = \underline{\underline{884 \text{W.m}^{-2}}}$$

A.2.2 Experiment 2

Condition: A₁ (0.5M CH₃OH), B₁ (Air), C₂ (Counter current), D₂ (Nafion® 211)



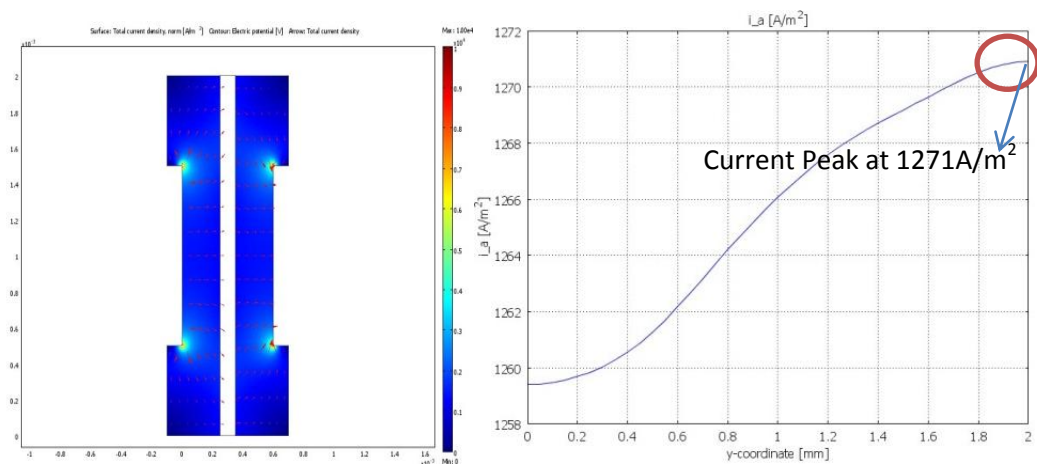
Current density peak generated in DMFC's experiment 1 is 1650A.m⁻²

Power Density: W= Current Density x Cell's Voltage

$$W = 1650 \text{A.m}^{-2} * 0.7 \text{V} = \underline{\underline{1155 \text{W.m}^{-2}}}$$

A.2.3 Experiment 3

Condition: A₁ (0.5M CH₃OH), B₂ (O₂), C₂ (Counter current), D₁ (Nafion® 117)



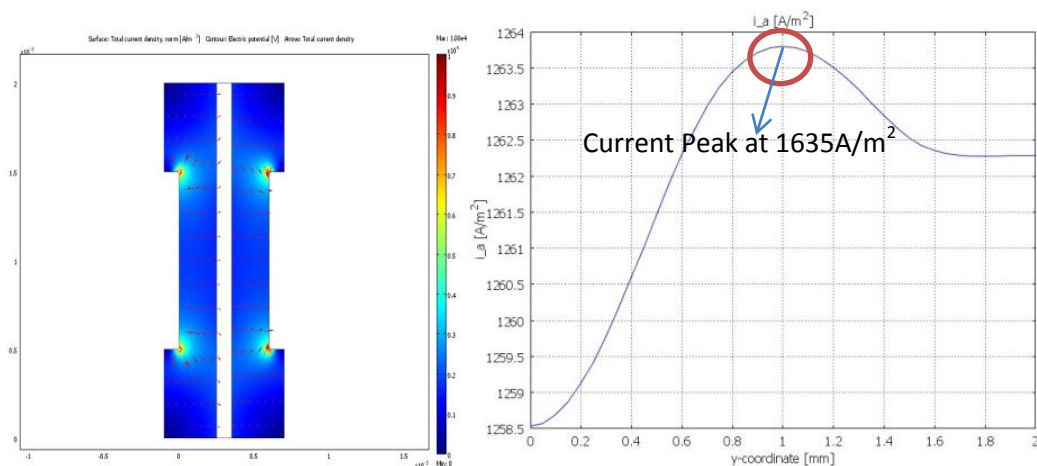
Current density peak generated in DMFC's experiment 1 is 1271A.m⁻²

Power Density: W= Current Density x Cell's Voltage

$$W = 1271 \text{A.m}^{-2} * 0.7 \text{V} = \underline{\underline{890 \text{W.m}^{-2}}}$$

A.2.4 Experiment 4

Condition: A₁ (0.5M CH₃OH), B₂ (O₂), C₁ (Concurrent), D₂ (Nafion® 211)



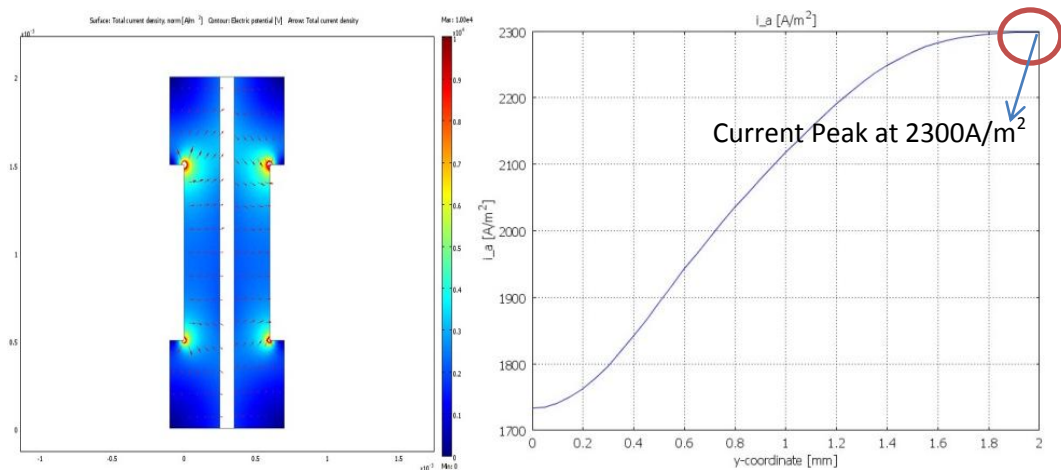
Current density peak generated in DMFC's experiment 1 is 1635A.m⁻²

Power Density: W= Current Density x Cell's Voltage

$$W = 1635 \text{A.m}^{-2} * 0.7 \text{V} = \underline{\underline{1145 \text{W.m}^{-2}}}$$

A.2.5 Experiment 5

Condition: A₂ (1 M CH₃OH), B₁ (Air), C₂ (Counter current), D₁ (Nafion® 117)



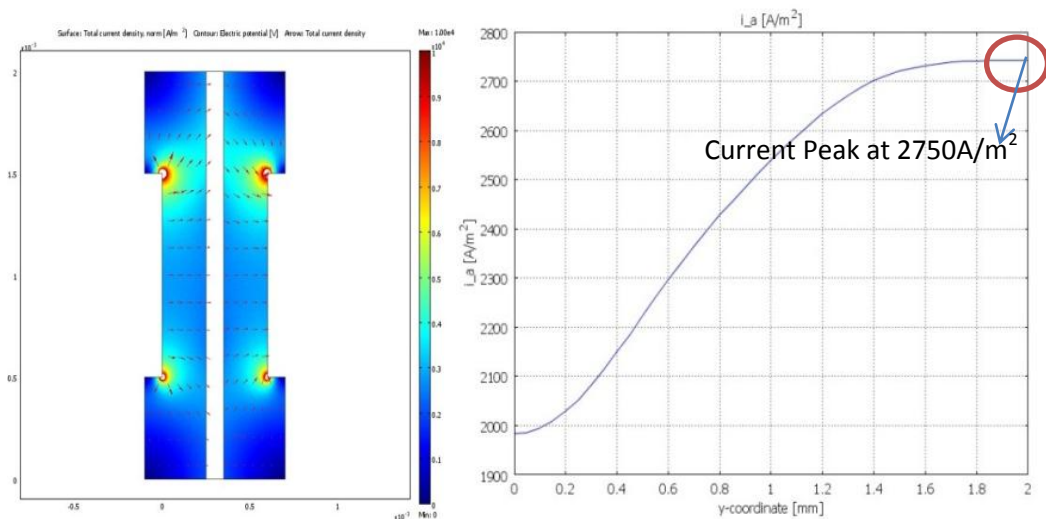
Current density peak generated in DMFC's experiment 1 is 2300A.m⁻²

Power Density: W= Current Density x Cell's Voltage

$$W = 2300\text{A.m}^{-2} * 0.7\text{V} = \underline{\underline{1610\text{W.m}^{-2}}}$$

A.2.6 Experiment 6

Condition: A₂ (1 M CH₃OH), B₁ (Air), C₁ (Concurrent), D₂ (Nafion® 211)



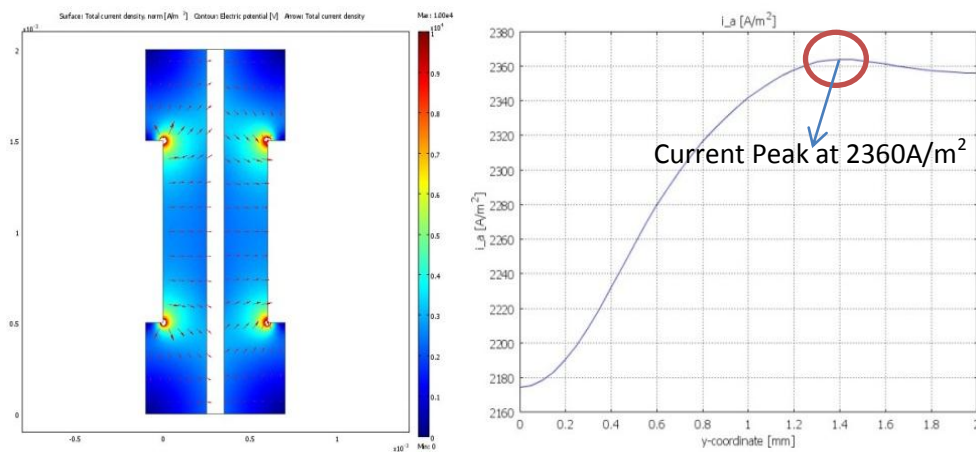
Current density peak generated in DMFC's experiment 1 is 2750A.m⁻²

Power Density: W= Current Density x Cell's Voltage

$$W = 2750\text{A.m}^{-2} * 0.7\text{V} = \underline{\underline{1925\text{W.m}^{-2}}}$$

A.2.7 Experiment 7

Condition: A₂ (1 M CH₃OH), B₂ (O₂), C₁ (Concurrent), D₁ (Nafion® 117)



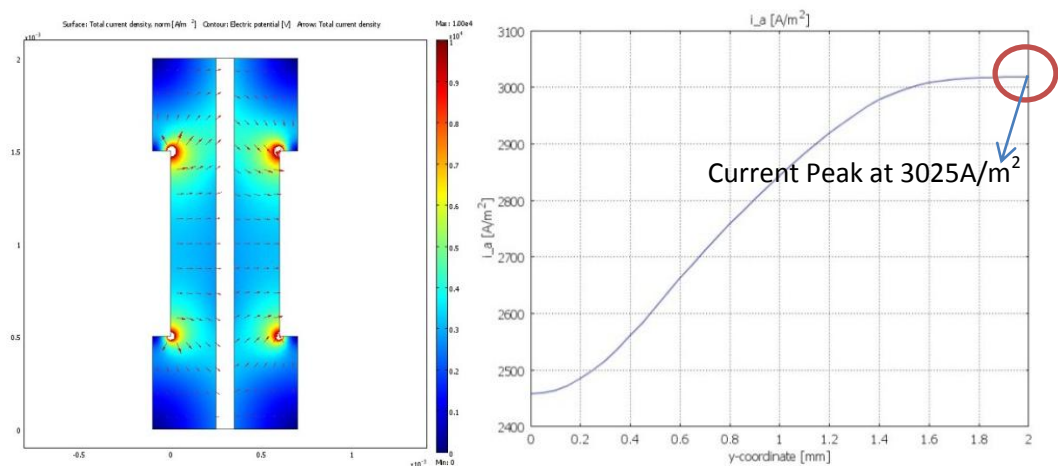
Current density peak generated in DMFC's experiment 1 is **2360A.m⁻²**

Power Density: $W = \text{Current Density} \times \text{Cell's Voltage}$

$$W = 2360 \text{A.m}^{-2} * 0.7 \text{V} = \underline{\underline{1652 \text{W.m}^{-2}}}$$

A.2.8 Experiment 8

Condition: A₂ (1 M CH₃OH), B₂ (O₂), C₂ (Counter current), D₂ (Nafion® 211)



Current density peak generated in DMFC's experiment 1 is **3025A.m⁻²**

Power Density: $W = \text{Current Density} \times \text{Cell's Voltage}$

$$W = 3025 \text{A.m}^{-2} * 0.7 \text{V} = \underline{\underline{2117 \text{W.m}^{-2}}}$$